Journal of Experimental Botany, Vol. 65, No. 6, pp. 1585–1603, 2014
doi:10.1093/jxb/eru016 Advance Access publication 18 February, 2014

Journal of Experimental Botany
www.jxb.oxfordjournals.org

RESEARCH PAPER

A plant spermine oxidase/dehydrogenase regulated by the proteasome and polyamines

Abdellah Ahou[1], Damiano Martignago[1], Osama Alabdallah[1], Raffaela Tavazza[2], Pasquale Stano[1], Alberto Macone[3], Micaela Pivato[4,5], Antonio Masi[4], Jose L. Rambla[6], Francisco Vera-Sirera[6], Riccardo Angelini[1], Rodolfo Federico[1] and Paraskevi Tavladoraki[1,*]

[1] Department of Science, University 'ROMA TRE', Rome, Italy
[2] Italian National Agency for New Technologies, Energy and Sustainable Economic Development (ENEA), UTAGRI-INN C.R. Casaccia, Rome, Italy
[3] Department of Biochemical Sciences 'A. Rossi Fanelli', University 'La Sapienza', Rome, Italy
[4] DAFNAE, University of Padova, Legnaro, Italy
[5] Proteomics Center of Padova University, Padova, Italy
[6] Instituto de Biología Molecular y Celular de Plantas, UPV-CSIC, Valencia, Spain

* To whom correspondence should be addressed. E-mail: paraskevi.tavladoraki@uniroma3.it

Received 31 October 2013; Revised 20 December 2013; Accepted 7 January 2014

Abstract

Polyamine oxidases (PAOs) are flavin-dependent enzymes involved in polyamine catabolism. In *Arabidopsis* five *PAO* genes (*AtPAO1–AtPAO5*) have been identified which present some common characteristics, but also important differences in primary structure, substrate specificity, subcellular localization, and tissue-specific expression pattern, differences which may suggest distinct physiological roles. In the present work, AtPAO5, the only so far uncharacterized AtPAO which is specifically expressed in the vascular system, was partially purified from *35S::AtPAO5-6His Arabidopsis* transgenic plants and biochemically characterized. Data presented here allow AtPAO5 to be classified as a spermine dehydrogenase. It is also shown that AtPAO5 oxidizes the polyamines spermine, thermospermine, and N^1-acetylspermine, the latter being the best *in vitro* substrate of the recombinant enzyme. AtPAO5 also oxidizes these polyamines *in vivo*, as was evidenced by analysis of polyamine levels in the *35S::AtPAO5-6His Arabidopsis* transgenic plants, as well as in a loss-of-function *atpao5* mutant. Furthermore, subcellular localization studies indicate that AtPAO5 is a cytosolic protein undergoing proteasomal control. Positive regulation of *AtPAO5* expression by polyamines at the transcriptional and post-transcriptional level is also shown. These data provide new insights into the catalytic properties of the *PAO* gene family and the complex regulatory network controlling polyamine metabolism.

Key words: Acetylated polyamines, dehydrogenase, polyamine oxidase, polyamines, spermidine, spermine, thermospermine.

Introduction

The polyamines putrescine (Put), spermidine (Spd), and spermine (Spm) are low molecular weight organic cations that are found in a wide range of organisms from animals to plants and bacteria, including thermophiles and diatoms that have a wider variety of polyamines, such as the Spm isomer thermospermine (Therm-Spm) and norspermine (Nor-Spm) as

Abbreviations: APAO, animal peroxisomal polyamine oxidase; AtPAO, *Arabidopsis thaliana* polyamine oxidase; Az, antizyme; CuAO, copper-containing amine oxidase; Dap, 1,3-diaminopropane; DCIP, 1,6 dichloroindophenol; DMSO, dimethylsulphoxide; GC-MS, gas chromatography–mass spectrometry; GUS, β-glucuronidase; H_2O_2, hydrogen peroxide; HPLC, high-performance liquid chromatography; LC-MS/MS, liquid chromatography–tandem mass spectrometry; Nor-Spm, norspermine; ODC, ornithine decarboxylase; PAO, polyamine oxidase; PDE, phosphodiesterase; Put, putrescine; SMO, spermine oxidase; Spd, spermidine; Spm, spermine; SSAT, spermidine/spermine N^1-acetyl-transferase; Therm-Spm, thermospermine; TLC, thin-layer chromatography.

well as long-chain and branched polyamines (Oshima, 2007; Morimoto *et al.*, 2010; Michael, 2011). They bind polyanionic macromolecules, such as DNA, RNA, and phospholipids, and are different from other multivalent cations, for example Mg^{2+}, in having a distributed charge whose spacing may allow them to interact more flexibly with the phosphates of DNA and RNA. Indeed, it is primarily through these ionic interactions with various important cellular anions that polyamines are believed to exercise their functions. Polyamines are also involved in various cellular processes through their further metabolism to various important cellular molecules, such as hypusinated translation initiation factor eIF5A (Chattopadhyay *et al.*, 2008), aldehydes and acrolein (Tavladoraki *et al.*, 2012), pantothenic acid (White *et al.*, 2001), γ-aminobutyric acid (Cona *et al.*, 2006; Kim *et al.*, 2013), various conjugates (Grienenberger *et al.*, 2009; Burrell *et al.*, 2012; Fellenberg *et al.*, 2012; Gaquerel *et al.*, 2013), alkaloids (Ober *et al.*, 2003), long-chain linear polyamines (Michael, 2011), and branched-chain polyamines (Oshima, 2007; Morimoto *et al.*, 2010). Moreover, hydrogen peroxide (H_2O_2) derived from polyamine catabolism has been shown to be involved in many physiological and pathological events (Babbar and Casero, 2006; Angelini *et al.*, 2010; Tavladoraki *et al.*, 2012; Cervelli *et al.*, 2013). In animals, polyamines contribute to a great number of cellular and physiological processes, such as cell division, proliferation and differentiation, gene expression, macromolecular synthesis, and apoptosis. In plants, polyamines are involved in growth and development, as well as in stress responses (Groppa and Benavides, 2008; Alcázar *et al.*, 2010; Mattoo *et al.*, 2010; Takahashi and Kakehi, 2010; Alet *et al.*, 2012), while in bacteria an essential role for polyamines in biofilm formation and adaptation to various stresses has been demonstrated (Lee *et al.*, 2009; Morimoto *et al.*, 2010).

To adjust polyamine levels finely to the levels required by the physiological state of the cell, various organisms have evolved complex homeostatic mechanisms involving polyamine biosynthesis, catabolism, transport, and uptake. Indeed, several endogenous and exogenous stimuli, as well as polyamines themselves induce changes in the expression levels of genes involved in polyamine metabolism through various regulatory mechanisms, which include modification of promoter activity and RNA stability, ribosomal frameshift and ribosome stalling, synthesis of inhibitory molecules, proteasome-mediated protein degradation, and substrate availability (Pegg, 2009; Fuell *et al.*, 2010; Ivanov *et al.*, 2010; Pegg and Michael, 2010). Among the biosynthetic enzymes, *S*-adenosylmethionine decarboxylase and ornithine decarboxylase (ODC) are highly regulated not only at the transcriptional but also at the post-transcriptional level. In particular, both animal and plant *S*-adenosylmethionine decarboxylases are subject to translational negative feedback regulation by polyamines which involves ribosome stalling due to the presence of upstream coding sequence 5′ of the main coding sequence (Law *et al.*, 2001; Hanfrey *et al.*, 2002, 2005; Raney *et al.*, 2002; Ivanov *et al.*, 2010). Furthermore, in animals, ODC is characterized by an extremely rapid intracellular turnover rate which is regulated by a small protein called antizyme (Az), whose synthesis is stimulated by polyamines through a ribosomal frameshift mechanism. Az inactivates ODC and targets it to ubiquitin-independent degradation by the 26S proteasome. Az itself is regulated by another ODC-related protein termed antizyme inhibitor which is highly homologous to ODC, but lacks ODC activity. The animal spermidine/spermine N^1-acetyltransferase (SSAT), a key enzyme in polyamine catabolism which adds acetyl groups to the aminopropyl end(s) of Spd and Spm, is also highly regulated at multiple levels, including transcription, mRNA processing, mRNA translation, and protein stabilization (Pegg, 2008). Interestingly, polyamines affect all of these steps. In particular, transcription and translation are increased in the presence of high levels of polyamines or polyamine analogues, whereas degradation of the SSAT protein though the 26S proteasome and incorrect splicing of the SSAT mRNA are reduced (Pegg, 2008).

Polyamine catabolism contributes greatly to polyamine homeostasis and is involved in several physiological processes (Angelini *et al.*, 2010). While Put is oxidized by copper-containing amine oxidases (CuAOs) to 4-aminobutanal with concomitant production of NH_3 and H_2O_2 in a terminal catabolic pathway (Tavladoraki *et al.*, 2012; Planas-Portell *et al.*, 2013), Spm as well as Spd and Therm-Spm are catabolized by polyamine oxidases (PAOs). PAOs are flavin-dependent enzymes (Angelini *et al.*, 2010; Tavladoraki *et al.*, 2012) which catalyse the oxidation of the free form and/or acetylated derivatives of polyamines at the secondary amino groups (Wang *et al.*, 2001; Wu *et al.*, 2003; Cona *et al.*, 2006). Animal peroxisomal PAOs (APAOs) preferentially oxidize N^1-acetyl-Spm, N^1-acetyl-Spd, and N^1,N^{12}-bis-acetyl-Spm at the carbon on the *exo*-side of N^4-nitrogen to produce Spd, Put, and N^1-acetyl-Spd, respectively, in addition to 3-acetamidopropanal and H_2O_2 (Landry and Sternglanz, 2003; Vujcic *et al.*, 2003; Wu *et al.*, 2003; Cona *et al.*, 2006). In contrast, the animal spermine oxidases (SMOs), which have a cytosolic/nuclear localization, preferentially oxidize the free form of Spm to produce Spd, 3-aminopropanal, and H_2O_2 (Wang *et al.*, 2001; Vujcic *et al.*, 2002; Cervelli *et al.*, 2003; Landry and Sternglanz, 2003). Thus, animal APAOs and SMOs are involved in a polyamine back-conversion pathway (Seiler, 2004).

In plants, the intracellular PAOs so far characterized (the *Arabidopsis thaliana* AtPAO1 with a putative cytosolic localization and the three peroxisomal enzymes AtPAO2, AtPAO3, and AtPAO4, as well as their orthologues in *Oryza sativa*) preferentially oxidize the free form of Spd or Spm to produce 3-aminopropanal, H_2O_2, and Put or Spd, respectively, the activity towards the acetylated polyamines being very low (Tavladoraki *et al.*, 2006; Moschou *et al.*, 2008; Kamada-Nobusada *et al.*, 2008; Fincato *et al.*, 2011; Ono *et al.*, 2012). Differently from the animal and plant intracellular PAOs, the extracellular PAO from *Zea mays* (ZmPAO1, previously ZmPAO; Tavladoraki *et al.*, 1998; Polticelli *et al.*, 2005) and its orthologues in *O. sativa*, *Avena sativa*, and *Hordeum vulgare* are involved in a terminal catabolic pathway oxidizing the carbon at the *endo*-side of the N^4-nitrogen of the free forms of Spd and Spm with the production of 4-aminobutanal and *N*-(3-aminopropyl)-4-aminobutanal, respectively,

in addition to 1,3-diaminopropane (Dap) and H_2O_2 (Cona *et al.*, 2006). Interestingly, the plant PAOs are characterized by a broad substrate specificity in that they are also able to oxidize the less abundantly found polyamines Therm-Spm and Nor-Spm (Tavladoraki *et al.*, 2006; Fincato *et al.*, 2011; Ono *et al.*, 2012) which in plants have an important role in vascular system differentiation and stress response (Kakehi *et al.*, 2008, 2010; Vera-Sirera *et al.*, 2010; Marina *et al.*, 2013). In contrast, murine SMO (MmSMO) was shown to be inactive with Therm-Spm (Fincato *et al.*, 2011).

In bacteria, such as *Pseudomonas aeruginosa*, *Citrobacter freundii*, and *Serratia marcescens*, which utilize polyamines as a source of carbon and nitrogen, Spd is oxidized by Spd dehydrogenases containing FAD and/or haem as prosthetic groups (Tabor and Kellog, 1970; Hisano *et al.*, 1990, 1992; Dasu *et al.*, 2006). Interestingly, reaction products of these enzymes with Spd are Dap and 4-aminobutanal, indicating a cleavage site at the *endo*-side of the N^4-nitrogen, while reaction products of the *P. aerugonosa* enzyme with Spm are Spd and 3-aminopropanal, indicating an *exo*-side mode of substrate cleavage (Tabor and Kellog, 1970; Okada *et al.*, 1979; Hisano *et al.*, 1992; Dasu *et al.*, 2006). It has been suggested that the position of the cleavage is determined by the structure of the substrate (Okada *et al.*, 1979).

In *A. thaliana*, there are five PAO genes (*AtPAO1*–*AtPAO5*) which present some common characteristics, but also important differences in primary structure, substrate specificity, subcellular localization, and expression pattern, differences which may reflect differences in physiological roles (Fincato *et al.*, 2011, 2012). In the present study, information was obtained about the catalytic properties of AtPAO5, the only so far uncharacterized *Arabidopsis* PAO, which allows this enzyme to be proposed as a spermine dehydrogenase. Data about the subcellular localization of AtPAO5 and regulation of gene expression were also obtained which show that AtPAO5 is regulated by the proteasomal pathway at the post-transcriptional level and by polyamines at the transcriptional and post-transcriptional level. This study may contribute greatly to a broader understanding of the function of plant PAOs.

Materials and methods

Sequence data

The amino acid sequences of PAOs were retrieved from the National Center for Biotechnology Information (NCBI) database based both on sequence annotation and sequence similarity. Sequence similarity searches were performed through BLASTP using the amino acid sequence of AtPAO1, AtPAO2, AtPAO3, AtPAO4, AtPAO5, and ZmPAO1 as queries. Multiple sequence alignment of the amino acid sequences was done using the program CLUSTALW2 and CLUSTAL OMEGA.

Plant growth conditions and treatments

All experiments were performed with *A. thaliana* ecotype Columbia. The seeds were first sterilized and stratified for 3 d at 4 °C and then put on agar plates containing half-strength Murashige and Skoog basal medium with Gamborg's vitamins and 0.5% (w/v) sucrose (1/2MS). Seedlings were grown in the growth chamber at 23 °C and under a 16 h light/8 h dark photoperiod. For quantitative reverse transcription–PCR (qRT–PCR) and western blot analysis following treatment with the proteasomal inhibitors MG132 and MG115 or the polyamines Spd and Spm, 7-day-old seedlings grown on 1/2MS agar plates were transferred to 1/2MS liquid medium and were grown a further 6 d. Following addition of fresh medium, seedlings were treated with 40 µM MG132 (Sigma-Aldrich) or MG115 (Sigma-Aldrich) from a stock of 10 mM dissolved in dimethylsulphoxide (DMSO) for 16 h. To avoid MG132 precipitation, the MG132 stock and the 1/2MS medium were pre-heated at 42 °C for 2 min before mixing. As a vehicle control, plants were treated with 0.4% (v/v) DMSO. For polyamine treatment, 0.2 M stocks in H_2O were used which were diluted to a final concentration of 0.5 mM.

Construction and characterization of transgenic plants

To obtain *35S::AtPAO5-6His*, *35S::AtPAO5-GFP*, and *35S::GFP-AtPAO5* transgenic plants the *AtPAO5* cDNA was amplified by PCR from plasmid *AtPAO5-pET17b* (Fincato *et al.*, 2011) in such a way as to permit the construction of the corresponding fusion genes via Gateway technology using the binary vectors *pK2GW7*, *pK7FWG2*, and *pK7WGF2*, respectively (Karimi *et al.*, 2002). The resulting constructs were used to transform *A. thaliana* wild-type plants by the *Agrobacterium tumefaciens* (strain GV301)-mediated floral dip transformation method as described by Clough and Bent (1998). At least 10 transgenic lines per construct, selected by kanamycin resistance and PCR analysis, were examined for transgene expression levels by RT–PCR and western blot analysis. An *Arabidopsis* T-DNA insertional mutant for the *AtPAO5* gene (*atpao5*) obtained from the Syngenta Arabidopsis Insertion Library (allele SAIL_664_A11.v1 for *AtPAO5*; Sessions *et al.*, 2002) was analysed for the presence of the T-DNA insertion by PCR, and homozygous mutant plants were selected. The lack of *AtPAO5*-specific mRNA in the homozygous mutant line was confirmed by RT–PCR.

Quantitative RT–PCR analysis

Total RNA was isolated from whole *Arabidopsis* seedlings using the RNeasy Plant Mini kit (QIAGEN). To degrade genomic DNA, DNase digestion was performed during RNA purification using the RNase-Free DNase Set (QIAGEN). For qRT–PCR analysis, cDNA synthesis and PCR amplification were carried out using GoTaq® 2-Step RT-qPCR System200 (Promega) according to the manufacturer's protocol. The PCRs were run in a Corbett RG6000 (Corbett Life Science, QIAGEN) utilizing the following program: 95 °C for 2 min and then 40 cycles of 95 °C for 7 s and 60°C for 40 s. The gene for ubiquitin-conjugating enzyme 21 (*UBC21*; *At5g25760*) was chosen as a reference gene using the oligonucleotides UBC21-for (5′-CTGCGACTCAGGGAATCTTCTAA-3′; Czechowski *et al.*, 2005) and UBC21-rev (5′-TTGTGCCATTGAA TTGAACCC-3′; Czechowski *et al.*, 2005). For qRT–PCR analysis of *AtPAO5*, *green fluorescent protein (GFP)*, and *β-glucuronidase (GUS)* expression levels, the oligonucleotides AtPAO5-qPCR-for (5′-GAGA GTGAGTATCAGATGTT TCCAG-3′), AtPAO5-qPCR-rev (5′-AG CACACCTAAAGAG ACAGTAACAA), EGFPfor, (5′-GGTGAG CAAGGGCGA GGAGCTGTTC-3′), EGFPrev, (5′-GTCGTCCTT GAAGAAGATGGTGCGCTC-3′), GUS-qPCR-for (5′-TCTGGTA TCAGCGC GAAGTC-3′), and GUS-qPCR-rev (5′-CCGT AATGA GTGACCGCATC-3′) were used. Fold change in the expression levels was calculated according to the ΔΔCq method.

Protein extraction from Arabidopsis *plants*

Plants grown either *in vitro* or in soil were homogenized initially with liquid nitrogen and then with protein extraction buffer containing 100 mM TRIS-HCl, pH 7.5, 0.2% (w/v) polyvinylpyrrolidone, 10% (v/v) glycerol and supplemented with 1 mM of the protease inhibitor phenylmethylsulphonyl fluoride. Crude protein extracts

were centrifuged at 13 000 *g* at 4 °C for 30 min and the clear supernatants were used either for western blot analysis after normalization for protein content or for recombinant AtPAO5 purification. Protein concentrations were determined by the method of Bradford using the Bio-Rad Protein Assay kit and bovine serum albumin as a standard.

Purification of recombinant AtPAO5 from transgenic Arabidopsis *plants by affinity chromatography*

Protein extracts from the *Arabidopsis 35S::AtPAO5-6His* transgenic plants were applied to Ni^{2+}-charged Sepharose (GE Healthcare) equilibrated with extraction buffer. The resin was washed first with extraction buffer and then with 100 mM TRIS-HCl, pH 7.5, 10% (v/v) glycerol, 10 mM imidazole. Recombinant protein was eluted with 300 mM imidazole, 100 mM TRIS-HCl, pH 7.5, 10% (v/v) glycerol, and dialysed against 50 mM TRIS-HCl, pH 8.0, 10% (v/v) glycerol using centrifugal filter devices (Millipore). The purification product was analysed by SDS–PAGE and Coomassie staining. Electrophoretic homogeneity was calculated by Image J analysis of the electrophoretic profile. Using this purification protocol, a yield of ~8 µg of recombinant enzyme per gram fresh weight was obtained.

Spectrophotometry and spectrofluorometry

Absorption spectra were measured by an Agilent 8453 diode-array spectrophotometer by using a 1 cm quartz microcuvette (sample volume 60 µl). Fluorescence measurements were performed on a JASCO FP-6200 spectrofluorometer by using a squared 0.3 cm quartz microcuvette (sample volume 60 µl). Excitation spectra were measured with fixed emission at 530 nm and emission spectra with excitation at 450 nm. Excitation and emission slit widths were set at 5 nm and spectra were recorded under high sensitivity conditions with a scan rate of 250 nm min^{-1}.

Cofactor analysis

Purified recombinant AtPAO5 was denatured either by addition of 6 M guanidine hydrochloride or by boiling for 15 min in the dark. Denatured protein was removed by centrifugation and the excitation/emission spectra of the supernatants were recorded. To discriminate between FAD and FMN, the fluorimetric-based method described by Aliverti *et al.* (1999) was employed. For the fluorimetric-based method, which exploits the fact that fluorescence of a FMN solution is 10-fold higher than that of a FAD solution, the cofactor released by protein boiling was treated with 15×10^{-3} U ml^{-1} of phosphodiesterase (PDE), which converts FAD into FMN, and changes in fluorescence intensity were quantified. To determine flavin content in recombinant AtPAO5, the fluorescence of denatured protein was quantified using a FAD titration curve. Flavin content was also determined by the absorption spectra considering an $\varepsilon_{458}=10.4 \times 10^3$ M^{-1} cm^{-1}).

Enzymatic activity assays

The catalytic activity of recombinant AtPAO5 with Spd, Spm, N^1-acetyl-Spm, Therm-Spm, and Nor-Spm was determined from purified protein by following spectrophotometrically the formation of a pink adduct ($\varepsilon_{515}=2.6 \times 10^4$ M^{-1} cm^{-1}) as a result of oxidation of 4-aminoantipyrine and 3,5-dichloro-2-hydroxybenzenesulphonic acid catalysed by horseradish peroxidase (Rea *et al.*, 2004) in 50 mM TRIS-HCl buffer, pH 6.5–8.5, at 25 °C. In this assay, for accurate measurements of low reaction rates in quartz cuvettes, care was taken to switch off the spectrophotometer deuterium (UV) lamp. To test catalytic activity in the presence of ferricenium hexafluorophosphate as an electron acceptor, a reaction mixture containing varying concentrations (200 µM to 1 mM) of ferricenium hexafluorophosphate in 50 mM TRIS-HCl buffer, pH 7.5 and 4 mM Spm was used and the decrease in absorbance at 300 nm was monitored ($\varepsilon_{300}=4.3 \times 10^3$ $M^{-1}cm^{-1}$; Lehman and Thorpe, 1990). Activity with potassium ferricyanide was determined using various concentrations of this electron acceptor (200 µM to 1 mM) in 50 mM TRIS-HCl buffer, pH 7.5 and measuring the decrease in absorbance at 420 nm ($\varepsilon_{420}=1.02 \times 10^3$ M^{-1} cm^{-1}). For activity with 1,6 dichloroindophenol (DCIP), reactions contained 150 µM or 300 µM DCIP in 50 mM TRIS-HCl buffer, pH 7.5 and the decrease in absorbance at 605 nm ($\varepsilon_{605}=12.5 \times 10^3$ M^{-1} cm^{-1} at pH 7.5) was measured. All assays were performed in the presence of O_2 at the air-saturated level (~237 µM; Wu *et al.*, 2003). Since ferricenium and ferricyanide are one-electron acceptors, for comparative analysis of catalytic constants, apparent k_{cat} values calculated at 500 µM ferricenium and ferricyanide (double that of the air-saturated levels of O_2 in solutions) were taken into consideration. For DCIP, apparent k_{cat} values at a concentration of 250 µM were taken into consideration.

Western blot analysis

Western blot analysis was performed utilizing a rabbit anti-6His tag polyclonal antibody conjugated to peroxidase (Abcam), a rabbit anti-GFP polyclonal antibody (Abcam), or a mouse anti-ubiquitin monoclonal antibody (Santa Cruz). For western blot analysis with anti-6His tag and the anti-GFP antibody, proteins were blotted to nitrocellulose whereas with anti-ubiquitin antibody proteins were blotted to a polyvinylidene fluoride (PVDF) membrane which was treated as described by Penengo *et al.* (2006). Detection of the labelled proteins was done with a chemiluminescence kit from Cyanagen or GE Healthcare.

Extraction of total free polyamines from plants

Total free polyamine levels were determined in whole *Arabidopsis* seedlings. For polyamine extraction, fresh plant material was homogenized initially with liquid nitrogen and then with cold 0.2 M $HClO_4$ (3 ml g^{-1} fresh weight). Crude extracts were incubated at 4 °C for 18 h and then clarified by centrifugation. The supernatants were analysed for polyamine content by high-performance liquid chromatography (HPLC) following addition of 80 µM 1,7-diaminoheptane as an internal standard and derivatization with dansyl chloride, or by gas chromatography–mass spectrometry (GC-MS) following addition of 8.6 µM 1,6 diaminohexane as an internal standard.

Analysis of Spm and N^1*-acetyl-Spm oxidation products by recombinant AtPAO5*

Reaction mixtures of 500 µl containing 50 mM TRIS-HCl pH 7.5, 2 µM purified recombinant AtPAO5, and 2 mM Spm or N^1-acetyl-Spm were prepared. Aliquots of 150 µl of the reaction mixtures were removed at various time intervals and analysed for polyamine content after addition of 0.2 M $HClO_4$. Following derivatization with dansyl chloride, polyamines were analysed by HPLC or thin-layer chromatography (TLC). For HPLC analysis, 1,7-diaminoheptane (80 µM) was added to the polyamine extracts before derivatization to be used as an internal standard. HPLC analysis was performed as previously described by Fincato *et al.* (2011).

Analysis of polyamine levels by GC-MS

Polyamines were analysed by GC-MS according to the method of Paik *et al.* (2006) with slight modifications. Briefly, aliquots of 0.5 ml of plant extracts in 0.2 M HClO4 were spiked with internal standard 1,6-diaminohexane (final concentration 8.6 µM) and adjusted to pH ≥12 with 0.5 ml of 5 M NaOH. The samples were then subjected to sequential *N*-ethoxycarbonylation and *N*-pentafluoropropionylation. *N*-Ethoxycarbonylation was performed in one step by adding to the aqueous phase ethyl

chloroformate (20 µl) in dichloromethane (1 ml). After vortex mixing for 2 min, the mixture was saturated with NaCl and extracted with 3 ml of diethyl ether and 2 ml of ethyl acetate in sequence. The organic phases were combined and dried under reduced pressure. The sample was then subjected to the second derivatization step by adding 20 µl of pentafluoropropionyl anhydride at 60 °C for 60 min. GC-MS analyses were performed with an Agilent 6850A gas chromatograph coupled to a 5973N quadrupole mass selective detector (Agilent Technologies, Palo Alto, CA, USA). Chromatographic separations were carried out with an Agilent HP-5ms fused-silica capillary column (30 m×0.25 mm id) coated with 5% phenyl–95% dimethylpolysiloxane (film thickness 0.25 µm) as stationary phase. Injection mode: splitless at a temperature of 260 °C. Column temperature program: 70 °C for 2 min and then to 300 °C at a rate of 15 °C min^{-1} and held for 5 min. The carrier gas was helium at a constant flow of 1.0 ml min^{-1}. The spectra were obtained in the electron impact mode at 70 eV ionization energy; ion source 280 °C; ion source vacuum 10^{-5} Torr. Mass spectrometric analysis was performed simultaneously in TIC (mass range scan from *m/z* 50 to 800 at a rate of 0.42 scans s^{-1}) and SIM mode. For GC-SIM-MS, the following quantitation ions were selected for each of the five polyamines analysed (Put, *m/z* 405; Spd, *m/z* 580, N^1-acetyl-Spm, *m/z* 637; Spm, *m/z* 709; Therm-Spm, *m/z* 391).

In-gel digestion, LC-MS/MS protein identification, and database search

The bands corresponding to AtPAO5 were excised from the gels, destained in 100 mM NH_4HCO_3, 50% acetonitrile for 30 min, dehydrated with acetonitrile, and dried in a SpeedVac. Cysteines were reduced with 10 mM dithiothreitol in 50 mM NH_4HCO_3 for 1 h at 56 °C and alkylated with 55 mM iodoacetamide for 45 min at room temperature in the dark. Gel pieces were consecutively washed with 50 mM NH_4HCO_3 and acetonitrile, and then dried. Proteins were *in situ* digested with sequencing grade modified trypsin (Promega, Madison, WI, USA) by adding 10 µl of the enzyme (12.5 ng $µl^{-1}$ trypsin in 25 mM NH_4HCO_3) to each band. Samples were incubated at 37 °C overnight. The peptides obtained were extracted three times with 50 µl of 50% (v/v) acetonitrile, 1% formic acid, dried under a vacuum, and dissolved in 10 µl of 0.1% (v/v) formic acid. Liquid chromatography–tandem mass spectrometry (LC-MS/MS) analyses were conducted with an LTQ-Orbitrap XL mass spectrometer (Thermo Fisher Scientific, Pittsburgh, CA, USA) coupled online with a nano-HPLC Ultimate 3000 (Dionex-Thermo Fisher Scientific). Samples (2 µl) were loaded onto a homemade 10 cm chromatographic column packed into a pico-frit (75 µm id, 10 µm tip, New Objectives) with C18 material (Aeris Peptide 3.6 u XB-C18 bulk packing, Phenomenex). Peptides were eluted with a linear gradient of acetonitrile, 0.1% formic acid from 3% to 50% in 45 min at a flow rate of 250 nl min^{-1}. Capillary voltage was set at 1.5 kV and source temperature at 200 °C. The MS2 acquisition method was based on a full-scan on the Orbitrap with a resolution of 60 000, followed by the MS/MS scans on the 10 most intense ions performed in the linear ion-trap. Raw data files were analysed against the ARATH Uniprot database (last update 2013_09, 33 340 sequences) with the software Proteome Discoverer 1.4 (ThermoFisher Scientific) interfaced to a Mascot search engine (version 2.0). Enzyme specificity was set to trypsin with two missed cleavages. The mass tolerance window was set to 10 ppm for parent mass and to 0.6 Da for fragment ions. Carbamidomethylation of cysteine and methionine oxidation residues were set as fixed modification and variable modifications, respectively. A false discovery rate (FDR) of 0.5% was calculated by Proteome Discoverer based on the search against the corresponding randomized database. Proteins with at least two peptides and significant confidence (P<0.05) were considered as having been positively identified.

Preparation of protoplasts from Arabidopsis *plants*

Protoplasts were prepared from leaves of *Arabidopsis* plants grown *in vitro* for 30 d. Leaf slices were incubated with K3 solution (Gamborg's complete basal medium, B5 vitamins, 36.92 g l^{-1} sucrose, 250 mg l^{-1} xylulose, 250 mg l^{-1} NH_4NO_3, 750 mg l^{-1} $CaCl_2$ $2H_2O$, 63 mg l^{-1} $CaHPO_4{\cdot}2H_2O$, 22.42 mg l^{-1} $NaH_2PO_4{\cdot}H_2O$, 1 mg l^{-1} naphthalene acetic acid, 0.2 mg l^{-1} 6-benzylaminopurine, 0.1 mg l^{-1} 2,4-dichlorophenoxyacetic acid; pH 5.6) at 26 °C for 1 h in the dark and then digested in the same solution supplemented with 2% (w/v) cellulase Onozuca R-10, 0.5% (w/v) dryselase, 0.25% (w/v) macerozyme R-10 overnight in the dark at 26 °C. Released protoplasts were filtrated through filters with a pore size of 88 µm and centrifuged at 100 *g* for 10 min. Floatated protoplasts were pelleted in washing medium (9 g l^{-1} NaCl, 18 g l^{-1} $CaCl_2{\cdot}2H_2O$, 0.4 g l^{-1} KCl, 1 g l^{-1} glucose; pH 5.7) and then resuspended in washing medium at a concentration of 10^6 protoplasts ml^{-1}. Protoplasts in washing medium were treated with 40 µM MG132 or 0.4% (v/v) DMSO (vehicle control) for 16 h and then observed under the confocal microscope.

Confocal microscopy analysis and imaging

For confocal analysis of *35S::AtPAO5-GFP* and *35S::GFP-AtPAO5 Arabidopsis* transgenic plants, 7-day-old seedlings grown in agar plates were transferred in 1/2MS liquid medium and left to grow for 24 h in the presence or absence of MG132, MG115, or DMSO under low light conditions. Confocal images were acquired with a Leica TCS-SP5 confocal microscope using the software Advanced Fluorescence (LAS AF; Leica). GFP fluorescence emission was detected between 505 nm and 525 nm with excitation at 488 nm with an argon laser and chlorophyll autofluorescence between 644 nm and 726 nm. For FM4-64 staining, detached *Arabidopsis* leaves were submerged in 5 µM FM4-64 (Molecular Probes) in 1/2MS medium for 15 min. Leaves were rinsed in distilled water and observed immediately. FM4-64 fluorescence was collected between 610 nm and 625 nm with excitation at 488 nm. For staining of mitochondria, protoplasts were incubated with mitoTracker® Red CM-H2XRos at a concentration of 500 nM for 30 min. Following washing, mitoTracker fluorescence was detected between 595 nm and 605 nm with excitation at 594 nm using an He–Ne laser. To determine root vascular differentiation, roots were stained with propidium iodide and observed under a confocal microscope at 543 nm (He–Ne laser) to measure the distance of the first protoxylem cells with secondary cell wall thickening from the quiescent centre.

Histochemical GUS analysis of AtPAO5::GFP-GUS Arabidopsis *transgenic plants*

Staining for GUS activity in *Arabidopsis* plants was performed essentially as described by Fincato *et al.* (2012). The reaction was allowed to proceed for 30 min to 1 h at 37 °C. Chlorophyll was extracted by several washes with ethanol:acetic acid (3:1, v/v). Samples were kept in 70% ethanol. Images were acquired by a Leica DFC420 digital camera applied to an Olympus BX51 microscope, and the distance between the first protoxylem cells with secondary cell wall thickening and the quiescent centre was measured by Image J analysis.

Results

AtPAO5 has higher sequence similarity to animal PAOs than to plant PAOs

Since several attempts to express *AtPAO5* functionally in various heterologous systems have been unsuccessful (Fincato *et al.*, 2011), the *AtPAO5* sequence was analysed to determine whether *AtPAO5* is indeed a functional PAO orthologue. Analysis of the genomic sequence evidenced that the *AtPAO5* gene bears no intron, in contrast to the other *AtPAO* genes and *ZmPAO1* which have eight introns (Fincato *et al.*, 2011). Although the lack of introns is one

of the characteristics of the processed pseudogenes, the possibility that *AtPAO5* is a pseudogene can be excluded on the basis of promoter activity studies and RT–PCR analysis. Indeed, characterization of *AtPAO5::GFP-GUS Arabidopsis* transgenic plants showed that the *AtPAO5* gene has a functional promoter (Fincato *et al.*, 2012). Furthermore, sequencing of the *AtPAO5* cDNA obtained by RT–PCR confirmed that *AtPAO5* produces a protein-coding mRNA of the correct size (data not shown). On the other hand, a ClustalW alignment of several PAO primary structures showed that the two regions of high similarity, one near the N-terminus and the other near the C-terminus, involved in flavin binding (Wu *et al.*, 2003), are highly conserved in AtPAO5 (Fig. 1), indicating that AtPAO5 is indeed a flavoprotein similar to the other plant and animal PAOs. The sequence alignment also showed that AtPAO5 has a higher sequence homology with MmSMO and murine APAO (MmAPAO) (31%) than with AtPAO1-4 and ZmPAO1 (19–23%) which instead have low sequence homology (20–25%) with the two mammalian enzymes.

The high similarity of the primary structure of AtPAO5 to those of MmSMO and MmAPAO extends not only to the flavin-binding domains, but also to the catalytic site. In particular, the MmSMO residues of the catalytic site His82, Tyr482, Ser527, Thr528, and Lys367 (Tavladoraki *et al.*, 2011) are conserved in AtPAO5 (Fig. 1). Among them, His82 has an important role in substrate binding (Tavladoraki *et al.*, 2011; Adachi *et al.*, 2012; Tormos *et al.*, 2012) and is conserved in most PAOs involved in polyamine back-conversion, such as, for example, MmAPAO, yeast FMS1, AtPAO2, AtPAO3, and AtPAO4, but not in AtPAO1 (Fig. 1). In contrast, the His82 residue is substituted by a glutamate residue in ZmPAO1, HvPAO1, and HvPAO2, enzymes involved in the terminal catabolism of polyamines.

The analysis of the AtPAO5 amino acid sequence also revealed the presence of four additional domains not present in the other four AtPAOs, MmSMO, and MmAPAO (Fig. 1). Instead, the MmSMO extra domain involved in nuclear targeting of the μ splicing variant of MmSMO (nuclear domain A; Cervelli *et al.*, 2004; Bianchi *et al.*, 2005) is absent in AtPAO5 (Fig. 1). In AtPAO5, two putative PEST motifs for protein degradation are also present, as shown by sequence analysis using the PESTFIND program (http://emboss.bioinformatics.nl/cgi-bin/emboss/epestfind). In particular, a domain with high probability to be recognized as a PEST motif is found near the N-terminus of the protein (amino acids 76–96), while a second one with lower probability is found in one of the AtPAO5 extra domains near the C-terminus of the protein (amino acids 420–435; Fig. 1). On the other hand, analysis of the AtPAO5 amino acid sequence by PSORT did not reveal the presence of any known targeting sequence to a specific subcellular compartment, thus suggesting cytosolic localization, similar to AtPAO1 (Tavladoraki *et al.*, 2006), but differently from AtPAO2–AtPAO4 which have a peroxisomal localization (Kamada-Nobusada *et al.*, 2008; Moschou *et al.*, 2008) and ZmPAO1 which has an extracellular localization (Cona *et al.*, 2006; Angelini *et al.*, 2010).

AtPAO5 *orthologues are widely distributed among the various plant taxa*

Similarity searches using the AtPAO5 amino acid sequence showed that *AtPAO5* orthologues are widely distributed among the various plant taxa. Indeed, the sequences of 23 *AtPAO5* orthologues present in several monocotyledonous (*Brachypodium distachyon*, *H. vulgare*, *O. sativa*, *Sorgum bicolor*, *Setaria italica* and *Z. mays*) and dicotyledonous plants (*Brassica juncea*, *Cicer arietinum*, *Cucumis sativus*, *Glycine max*, *Medicago truncatula*, *Populus trichocarpa*, *Prunus persica*, *Ricinus communis*, *Solanum lycopersicum*, and *Vitis vinifera*), as well as in the seedless ancient vascular plant *Selaginella moellendorffi* were retrieved from the databases (Supplementary Table S1 at *JXB* online). Conversely, no *AtPAO5* orthologue was found in the non-vascular plant *Physcomitrella patens*, or in gymnosperms for which, however, only few sequencing data are available so far. In a phylogenetic analysis, all *AtPAO5* orthologues appeared clustered together and separately from the orthologues of the other *AtPAO* genes. (P. Tavladoraki and D. Salvi, unpublished results). Furthermore, except for three *AtPAO5*-like genes in *C. sativus*, *G. max*, and *V. vinifera* (*CsPAO1*, *GmPAO9*, and *VvPAO7*, respectively), which have a single intron and an *AtPAO5*-like gene, in *S. lycopersicum* (*SlPAO4*), which has two introns, all other *AtPAO5* orthologues taken into consideration in the present study and for which genomic sequences are available bear no intron. On the other hand, the extra domains present in AtPAO5 in respect to the other AtPAOs, ZmPAO1, MmSMO, and MmAPAO, are present in almost all the AtPAO5-like proteins, though with a low degree of sequence similarity to each other. In addition, analysis of the amino acid sequence of the AtPAO5-like proteins showed the presence of putative PEST sequences not only in AtPAO5 but also in some other proteins, such as BjPAO, HvPAO5, OsPAO1, PrPAO1, SmPAO5, and SmPAO6 (data not shown).

Recombinant AtPAO5 is an FAD-dependent spermine dehydrogenase

To examine AtPAO5 catalytic activity, and since ectopic expression of this gene in heterologous systems (bacteria and yeast) has been unsuccessful under conditions used previously (Fincato *et al.*, 2011), in the present study overexpression of *AtPAO5* in a homologous system was attempted. In particular, *35S::AtPAO5-6His Arabidopsis* transgenic plants, with the sequence of the 6-His tag at the 3′ end of the *AtPAO5* cDNA, were constructed. Among the various transgenic lines selected by kanamycin resistance, the one with the highest expression levels was used for purification of the recombinant protein through affinity chromatography. Indeed, using these plants, it became possible to purify a small amount of recombinant AtPAO5 with an apparent molecular mass of ~64 kDa, which is higher than that of recombinant ZmPAO1 (Fig. 2; Polticelli *et al.*, 2005), as expected from the amino acid sequence. However, despite an enrichment of >100-fold (Fig. 2B), the purification of the recombinant protein was only partial, as electrophoretic analysis of the final product showed

Fig. 1. Amino acid sequence alignment of plant and animal PAOs. Sequence alignment was performed with the program CLUSTALW2. The numbering of amino acid residues is shown on the right. In ZmPAO1, the peptide signal is underlined, and the numbering starts from the first amino acid residue of the mature protein. Residues of the ZmPAO1 catalytic site, as well as the corresponding residues conserved in other PAOs, are marked with red letters, while those of MmSMO are in violet. Identical amino acids with respect to AtPAO5 are highlighted in grey. Red boxes enclose putative PEST motifs. White characters identify the amino acids present in AtPAO5 extra domains (highlighted in blue) and MmSMO (highlighted in green). The sequences for peroxisomal targeting of AtPAO2 and MmAPAO are marked in green. AtPAO2 was chosen as the representative member of the AtPAO2–AtPAO4 subfamily. Lines above sequences represent flavin-binding sites. Red numbers in parentheses indicate the percentage of amino acid sequence identity to AtPAO5.

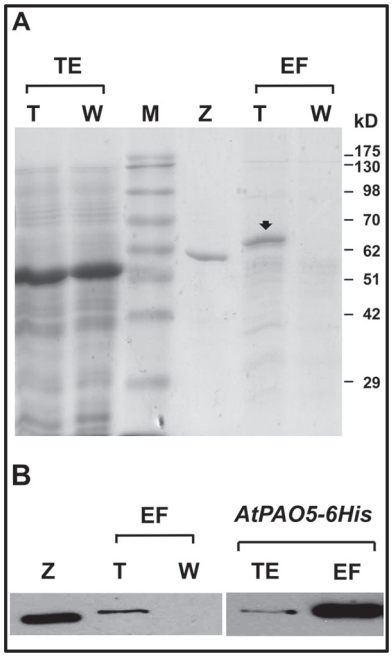

Fig. 2. Analysis of the recombinant AtPAO5 purified from *35S::AtPAO5-6His Arabidopsis* transgenic plants. SDS–PAGE (A) and western blot (B) analysis of total extracts (TE) and elution fractions (EF) of affinity column preparations from *35S::AtPAO5-6His* transgenic (T) and wild-type (W) *Arabidopsis* plants. The black arrow shows recombinant AtPAO5, as confirmed by western blot analysis. In the western blot analysis an anti-6His antibody was used. M, molecular mass marker (GeneDirex); Z, purified recombinant ZmPAO1 (Polticelli *et al.*, 2005). Numbers indicate the molecular mass of marker proteins.

(a calculated electrophoretic homogeneity of 70%; Fig. 2A). Since various attempts to increase the yield and purity of the recombinant protein were not successful, the AtPAO5-enriched preparations were used to obtain information about the spectral and catalytic properties of the recombinant protein.

The absorption spectrum of the recombinant enzyme provided evidence for the presence of flavin, presenting the two typical peaks of the oxidized flavin cofactor at 387 nm and 460 nm (Fig. 3A). This was further confirmed by analysis of the purified recombinant protein through spectrofluorometry. In particular, the fluorescence excitation spectrum of recombinant AtPAO5 again showed the two characteristic peaks of the flavin cofactor at 380 nm and 450 nm, while the emission spectrum exhibited a peak at 530 nm (Fig. 3B). These signals were absent in the corresponding spectra of control preparations from wild-type plants. Denaturation of recombinant AtPAO5 with 6 M guanidine hydrochloride or by boiling increased the intensity of the signals in the AtPAO5 excitation/emission spectra (Fig. 3B), implying that the apoprotein environment affects these spectra and that the cofactor is non-covalently bound in the recombinant enzyme. Furthermore, treatment of the denatured protein with PDE, which converts FAD to FMN (Aliverti *et al.*, 1999), induced a 10-fold increase in fluorescence intensity, indicating that FAD, and not FMN, is present in the recombinant protein. FAD quantification through analysis of absorption and emission spectra, and determination of protein content through Bradford and UV absorbance, allowed calculation of a mean value of 0.95 mole of FAD per mole of enzyme.

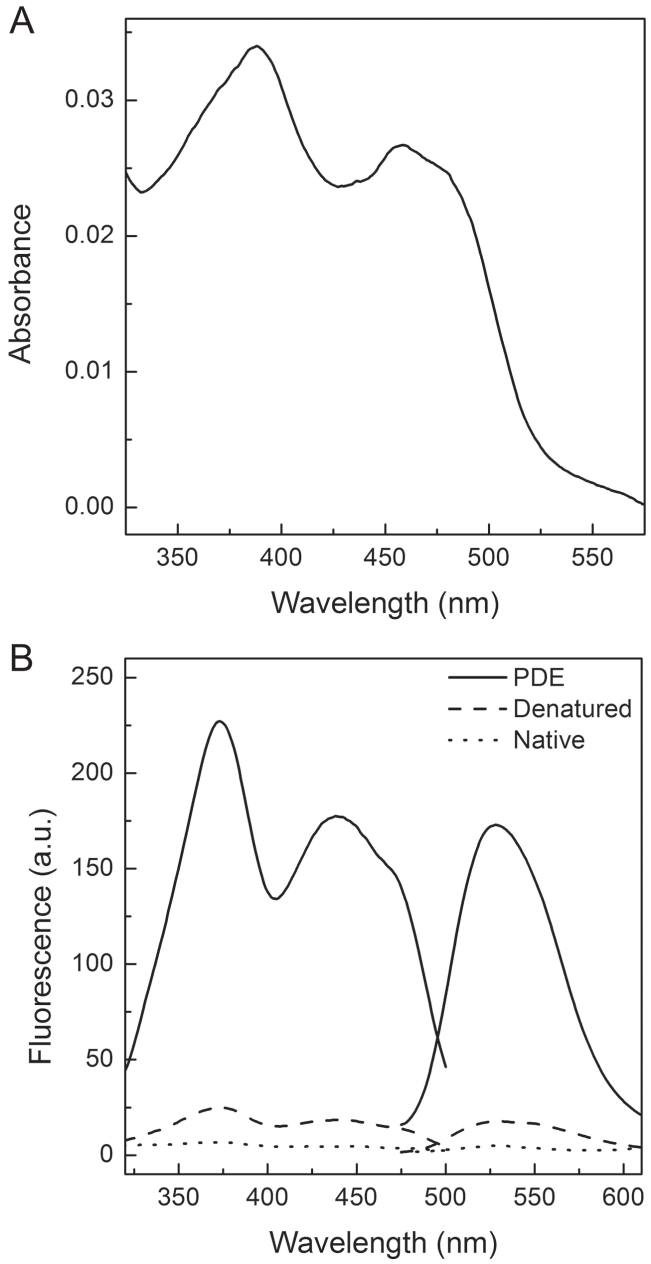

Fig. 3. Spectral analysis of purified recombinant AtPAO5. (A) Absorption spectrum of recombinant AtPAO5. (B) Fluorescence excitation (curves on the left) and emission spectra (curves on the right) of recombinant AtPAO5 under native conditions or following denaturation by boiling and centrifugation. Fluorescence excitation and emission spectra were also recorded following treatment of the released cofactor with phosphodiesterase (PDE).

Enzymatic activity assays showed the presence of PAO activity in the AtPAO5-enriched preparations from the *35S::AtPAO5-6His* transgenic plants, but not in the control preparations from wild-type *Arabidopsis* plants, indicating that the activity present in the enriched AtPAO5 preparation is specific for the recombinant protein. In particular, a peroxidase-coupled enzymatic assay revealed that recombinant AtPAO5 is active with Spm, Therm-Spm, N^1-acetyl-Spm, and Nor-Spm (Spm >N^1-acetyl-Spm ≥Therm-Spm ≥Nor-Spm; Table 1) with a pH optimum of 7.5–8.0. However, AtPAO5 was not active with Spd, similarly to AtPAO1 and MmSMO (Tavladoraki *et al.*, 2006; Fincato *et al.*, 2011).

A calculation of the turnover rate monitoring the H_2O_2 production by the peroxidase-coupled assay showed a k_{cat} with Spm of 1.1×10^{-2} s^{-1} which is much lower than that of other plant and animal PAOs and SMOs (ranging between 2 s^{-1} and 50 s^{-1}). To investigate whether this low k_{cat} value is due to poor reactivity of AtPAO5 with molecular oxygen to re-oxidize the reduced cofactor generated during the reductive half-reaction, the reactivity of AtPAO5 with alternative electron acceptors was investigated. In particular, ferricenium hexafluorophosphate, potassium ferricyanide, and DCIP, which have often been used as synthetic electron acceptors to assay for the activity of flavin-dependent oxidoreductases, were employed. Using the ferricenium-based assay, an apparent k_{cat} value with Spm of 1.9 s^{-1} was calculated (Table 1) which is ~180-fold higher than that with the peroxidase-coupled assay, thus indicating that O_2 is indeed a very poor acceptor of electrons in the reaction catalysed by recombinant AtPAO5. Conversely, similar assays performed with recombinant ZmPAO1 and MmSMO showed that ferricenium is a poorer electron acceptor than O_2 (k_{cat} values with ferricenium being 10% and 54% of that with O_2, respectively). Also using ferricyanide as an electron acceptor in the reaction of AtPAO5 with Spm, an apparent k_{cat} value of 1.3 s^{-1} was calculated, which is 118-fold higher than that with the peroxidase-coupled assay. DCIP was also shown to be a better electron acceptor than O_2 for AtPAO5, but poorer than ferricenium and ferricyanide (Table 1). These data suggest that AtPAO5 has a better activity as a dehydrogenase rather than as an oxidase. Surprisingly, using the ferricenium-based assay, it was determined that the k_{cat} value of AtPAO5 for N^1-acetyl-Spm is 3.3-fold higher than that for Spm, whereas with the peroxidase-coupled assay AtPAO5 was calculated to be half as active with N^1-acetyl-Spm than with Spm (Table 1). In a similar way, using the ferricenium-based assay, recombinant AtPAO5 was shown to be equally active with Spm and Therm-Spm, in contrast to the peroxidase-coupled assay with which recombinant AtPAO5 was calculated to be half as active with Therm-Spm as with Spm (Table 1). These data suggest that with the best electron acceptor, the best *in vitro* substrate for recombinant AtPAO5 is N^1-acetyl-Spm and that this enzyme also has a good activity with Therm-Spm.

Recombinant AtPAO5 is involved in polyamine back-conversion

To investigate the cleavage mode of recombinant AtPAO5, the reaction products from Spm and N^1-acetyl-Spm were analysed by both HPLC (Fig. 4) and TLC (Supplementary Fig. S1 at *JXB* online). These analyses showed the production of Spd and not Dap from both substrates. These data indicate that, similarly to the other four AtPAOs, AtPAO5 is involved in a polyamine back-conversion pathway and not in the terminal catabolism of polyamines. The lack of Put from the reaction products of recombinant AtPAO5 with Spm and N^1-acetyl-Spm is in agreement with the lack of activity of this enzyme with Spd.

AtPAO5 oxidizes the polyamines Spm, N^1-acetyl-Spm, and Therm-Spm in vivo

To determine the *in vivo* substrate preference of AtPAO5, the free soluble polyamine levels in the *35S::AtPAO5-6His* transgenic plants were determined by HPLC (data not shown) and GC-MS (Table 2), the latter technique being necessary for identification of Therm-Spm and N^1-acetyl-Spm. Indeed, using GC-MS, it became possible to quantify the levels of not only Therm-Spm, but also of N^1-acetyl-Spm in *Arabidopsis* plants, which appeared to be 10-fold lower than those of Spm and similar to those of Therm-Spm (Table 2). Until now, N^1-acetyl-Spm has been detected only in a few plant species, such as the subantarctic crucifer *Pringlea antiscorbutica* in which it is present at a similar concentration to that in *Arabidopsis* (Dufeu *et al.*, 2003; Hennion *et al.*, 2006). In *Arabidopsis*, the presence of only N^8-acetyl-Spd has been reported so far, while in maize that of N^1-acetyl-Spd has been shown (de Agazio *et al.*, 1995; Tassoni *et al.*, 2000).

The analysis of the polyamine levels by HPLC and GC-MS showed a statistically significant decrease of Spm, Therm-Spm, and N^1-acetyl-Spm levels in the *35S::AtPAO5-6His* transgenic plants as compared with the wild-type plants (Table 2), thus indicating that all three polyamines, Spm, Therm-Spm, and N^1-acetyl-Spm, are the physiological substrates of this enzyme. This was further confirmed through analysis of polyamine levels in a loss-of-function *atpao5* mutant. Indeed, in agreement with the data from the

Table 1. *Kinetic constants of recombinant AtPAO5 with various electron acceptors and various polyamines*

	Spm		Therm-Spm		N^1-Acetyl-Spm	
	k_{cat} (s^{-1})	*R*	k_{cat} (s^{-1})	*R*	k_{cat} (s^{-1})	*R*
O_2	$(1.1 \pm 0.5) \times 10^{-2}$	1	$(5.1 \pm 0.4) \times 10^{-3}$	0.5	$(4.6 \pm 0.6) \times 10^{-3}$	0.4
Ferricenium	1.9 ± 0.5	173	1.7 ± 0.3	154	6.2 ± 2.5	564
Ferricyanide	1.3 ± 0.7	118				
DCIP	$(2.8 \pm 0.3) \times 10^{-1}$	25				

All reactions were performed in 50 mM TRIS-HCl, pH 7.5 and in the presence of O_2 at the air-saturated level.
Apparent k_{cat} values determined in the presence of 500 μM ferricenium, 500 μM ferricyanide, or 250 μM 2,6 dichloroindophenol (DCIP) are also reported.
Results are mean values ±SE.
R, fold change of k_{cat} values with respect to the k_{cat} value for Spm with only O_2 as an electron acceptor.

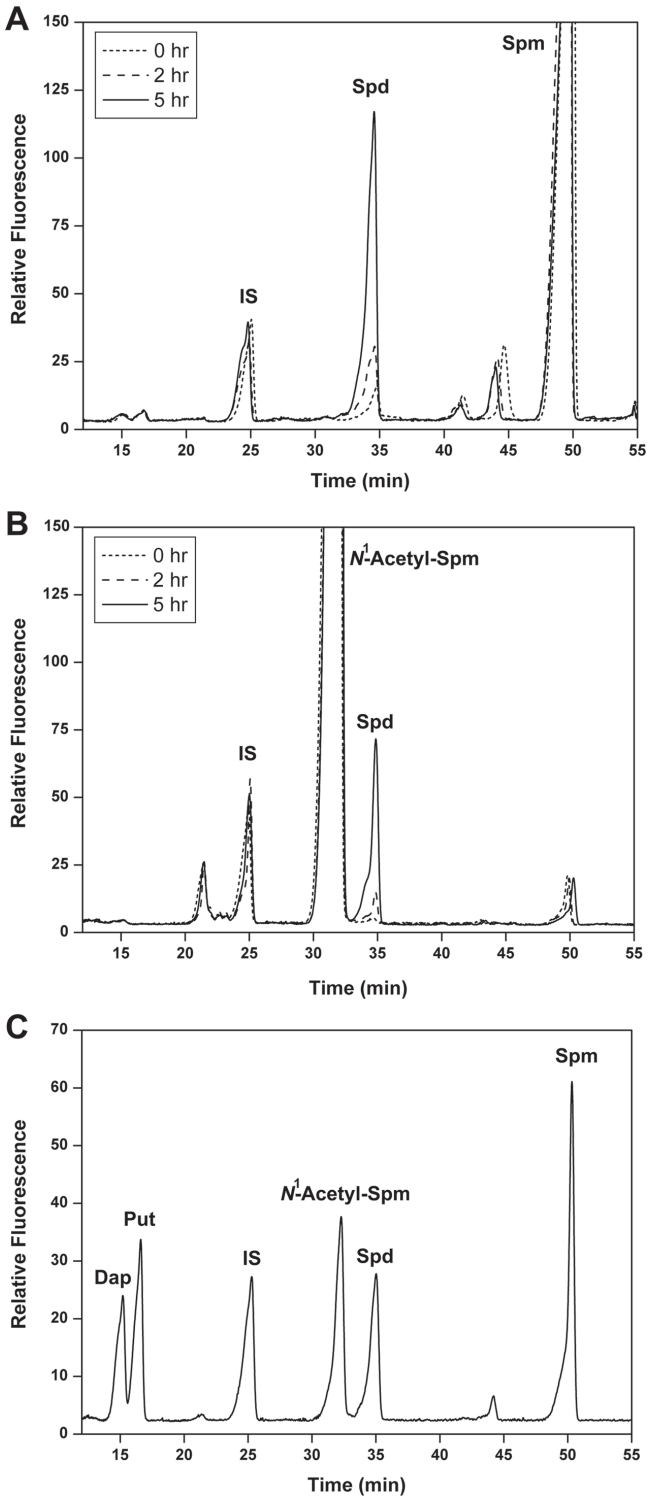

Fig. 4. Analysis of AtPAO5 reaction products from Spm and N^1-acetyl-Spm by HPLC. Purified recombinant AtPAO5 (2 μM) was incubated with 2 mM Spm (A) or N^1-acetyl-Spm (B). Reactions were allowed to proceed for 0, 2, and 5 h, and reaction products were analysed by HPLC following dansylation. (C) Chromatogram of a mixture of polyamines to indicate elution time. IS, 1,7 diaminoheptane used as an internal standard; Dap, 1,3 diaminopropane. Data are from a single representative experiment, which was repeated twice.

35S::AtPAO5-6His transgenic plants, the levels of the same three polyamines were significantly increased in the *atpao5* mutant plants compared with the wild-type plants (Table 2).

Studies on AtPAO5 subcellular localization

To confirm the cytosolic localization of AtPAO5, transgenic *Arabidopsis* plants expressing translational fusions between AtPAO5 and GFP were generated. To rule out mistargeting due to the presence of the reporter, GFP was appended either at the N- or the C-terminus of AtPAO5 (*35S::GFP-AtPAO5* and *35S::AtPAO5-GFP* transgenic plants, respectively). The different *35S::GFP-AtPAO5* and *35S::AtPAO5-GFP* transgenic lines were analysed for expression levels of transgenes by RT–PCR and western blot analysis. Comparative analysis of the best expressors between the independent *35S::GFP-AtPAO5* and *35S::AtPAO5-GFP* transgenic lines (transgenic lines A3 and B6, respectively) showed higher expression levels of the transgene in the *35S::GFP-AtPAO5* transgenic plants as compared with those in the *35S::AtPAO5-GFP* transgenic plants at both the mRNA and the protein level (Supplementary Fig. S2 at *JXB* online). In particular, it was calculated by both semi-quantitative (data not shown) and qRT-PCR (Supplementary Fig. S2A) that the *GFP-AtPAO5* transcript level in transgenic line A3 was 1.5-fold higher than that of the *AtPAO5-GFP* transcript in the transgenic line B6 with a 10-fold difference at the corresponding protein levels (Supplementary Fig. S2B). This suggests either a higher translational efficiency or increased protein stability of the recombinant *GFP-AtPAO5* with respect to the recombinant *AtPAO5-GFP*. Free GFP was not present either in the *35S::GFP-AtPAO5* or in the *35S::AtPAO5-GFP* transgenic plants, as shown by western blot analysis (data not shown), indicating that the two recombinant proteins accumulated in an intact form in the corresponding transgenic plants.

The *35S::GFP-AtPAO5* and *35S::AtPAO5-GFP* transgenic plants were analysed for the subcellular distribution of the GFP fluorescence using confocal microscopy. Analysis of *35S::AtPAO5-GFP* protoplasts and leaves showed the presence of intracellular GFP-related fluorescent spots (fluorescent bodies) of variable dimension (0.7–1.5 μm), number (1–5), and shape (Fig. 5A–D). These fluorescent bodies did not present co-localization with chloroplasts (Fig. 5A, B) and mitochondria (Fig. 5F–H). Furthermore, association of these protein bodies with peroxisomes can be excluded because of their number which was always low, in contrast to the high number of peroxisomes present in the leaves of the plants at the same developmental stage as the *35S::AtPAO5-GFP* plants, and did not display the characteristic intracellular movement of peroxisomes (Mano *et al.*, 2002). Indeed, parallel analysis of *35S::GFP-AtPAO3 Arabidopsis* transgenic plants overexpressing the peroxisomal GFP–AtPAO3 fusion protein (Moschou *et al.*, 2008; Fincato *et al.*, 2011) showed a large number of fluorescent peroxisomes undergoing rapid movement which made them appear rod shaped in the confocal images (Fig. 5P; red arrows).

In the case of *35S::GFP-AtPAO5* leaves and protoplasts, a GFP-related fluorescence was mainly observed at the cell periphery (Fig. 5I–L). This distribution of the fluorescence may represent *GFP-AtPAO5* localization in the cell wall, plasma membrane, tonoplast, or the thin layer of the cytoplasm that is between the plasma membrane and the tonoplast

Table 2. Polyamine levels (nmol g^{-1} fresh weight) in *35S::AtPAO5-6His* and *atpao5 Arabidopsis* plants

	Put	Spd	Spm	N^1-Acetyl-Spm	Therm-Spm
WT	99.8 ± 24.5	481.1 ± 10.3	29.5 ± 1.5	3.4 ± 0.3	3.7 ± 0.3
35::AtPAO5-6His	90.7 ± 10.5	431.5 ± 40.6	20.8 ± 5.2*	2.6 ± 0.3*	1.7 ± 0.4*
atpao5	79.1 ± 25.7	455.6 ± 37.2	35.8 ± 3.4*	4.3 ± 0.2*	6.8 ± 2.4*

The levels of Put, Spd, Spm, N^1-acetyl-Spm, and Therm-Spm were determined by GC-MS. The analysis was repeated twice (n=3).
Numbers are mean values ±SD. Statistical analysis was performed by one-way ANOVA test.
*Statistically significant differences ($P < 0.05$) with respect to the corresponding values in wild-type plants (WT).
Similar results for Put, Spd, and Spm were obtained by HPLC analysis of polyamine levels, which was repeated more than three times.

considering that plant cells typically contain a very large vacuole that accounts for most of the cell volume. However, the presence of the GFP–AtPAO5-related fluorescence in the freshly prepared protoplasts as well as the detachment of the GFP–AtPAO5 fluorescence from the cell wall together with the plasma membrane caused by plasmolysis (Fig. 5M) allow cell wall localization to be ruled out. Plasma membrane localization can also be excluded since the GFP–AtPAO5-related fluorescence did not completely overlap with the fluorescence of the membrane-specific marker FM4-64 (Fig. 5M, N). Furthermore, the often diffuse distribution (Fig. 5K, N) of the GFP–AtPAO5 fluorescence as well as its presence in cytoplasmic strands (Fig. 5J, M; yellow arrowheads) exclude localization to the tonoplast and suggest cytosolic localization. Indeed, the distribution of the GFP–AtPAO5 fluorescence resembles yellow fluorescent protein (YFP) distribution in the *35S::YFP* transgenic plants expressing YFP with no targeting sequence which is detected as a thick, patchy line circumventing the cell as well as in cytoplasmic strands and nuclei (Fig. 5O; Bloch *et al.*, 2005). Nevertheless, together with the diffused fluorescence distribution, AtPAO5–GFP-like fluorescent bodies were sometimes also observed in the *35S::GFP-AtPAO5* transgenic plants (Fig. 5K, yellow arrow).

AtPAO5 *expression is regulated by the proteasomal pathway*

To determine the nature of the fluorescent bodies observed in the *35S::GFP-AtPAO5* and *35S::AtPAO5-GFP* transgenic plants and considering that putative PEST motifs for protein targeting to the proteasomal machinery were identified in the AtPAO5 sequence, *35S::AtPAO5-GFP* and *35S::GFP-AtPAO5* seedlings and protoplasts were treated with the proteasomal inhibitor MG132 and then observed under a confocal microscope. MG132 is a potent and selective inhibitor of chymotrypsin-like proteolytic activity of the proteasome with no effect on earlier steps of the proteasomal pathway during which mono- or polyubiquitination of the target protein often occurs (Lee and Goldberg, 1998). In this way, MG132 treatment causes an increase in the accumulation levels of the proteins marked for degradation by the proteasome complex (Lee and Goldberg, 1998). Indeed, treatment for 16 h of the transgenic and wild-type *Arabidopsis* plants with MG132 increased the total amount of ubiquitinated proteins as shown by western blot analysis using an ubiquitin (UBQ)-specific antibody (Supplementary Fig. S3 at *JXB* online). Confocal analysis of *35S::AtPAO5-GFP* transgenic plants treated with MG132 revealed that this inhibitor induces an increase in the number of the cells presenting GFP-related fluorescent bodies (Fig. 6) both when protoplasts (Fig. 6A, B) and when leaves (Fig. 6C, D) were observed. MG132 also caused an increase in the number of the fluorescent bodies in the *35S::GFP-AtPAO5* transgenic plants (Fig. 6E, F),while no fluorescent body was detected in the *35S::YFP* transgenic plants treated or not with MG132 (Fig. 6G, H). Similar results were obtained using the proteasomal inhibitor MG115 (data not shown) which has the same mode of action as MG132 (Myung *et al.*, 2001).

The increase in the GFP–AtPAO5 and AtPAO5–GFP protein bodies caused by the two proteasomal inhibitors was further confirmed by western blot analysis of protein extracts from seedlings treated or not with MG132. Indeed, this analysis showed an increase in the amount of the two fusion proteins in the corresponding transgenic plants following treatment with the proteasomal inhibitor as compared with mock-treated transgenic plants (Fig. 7). Furthermore, MG132 treatment increased the levels of the AtPAO5-6His recombinant protein, but not of YFP recombinant protein in the *35S::AtPAO5-6His* and the *35S::YFP Arabidopsis* transgenic plants, respectively (Fig. 7), indicating that the effect of MG132 on the accumulation levels of the three AtPAO5 chimeric proteins is AtPAO5 specific and GFP independent. Instead, MG132 induced no change in the amount of the corresponding messengers, as shown by qRT–PCR (Supplementary Fig. S2A at *JXB* online). Altogether, these data suggest that AtPAO5 is a cytosolic protein found under the control of the proteasome and that the observed fluorescent protein bodies represent aggregated forms of the protein resulting from the proteasomal pathway.

As shown in Fig. 8, the proteasome inhibitor MG132 induced an increase in the amount of the recombinant AtPAO5 protein without altering its molecular weight. These results may suggest that recombinant AtPAO5 is not ubiquitinated. However, monoubiquitination could not be excluded by these data, since UBQ, being a small protein of 8.5 kDa, may have only a small effect on the mobility of the monoubiquitinated proteins, not detectable under certain experimental conditions. To verify this possibility, the bands corresponding to the purified recombinant AtPAO5-6His protein in the SDS–PAGE analysis of two distinct preparations were analysed by mass spectrometry. This analysis further confirmed the identity of the recombinant protein with a coverage of

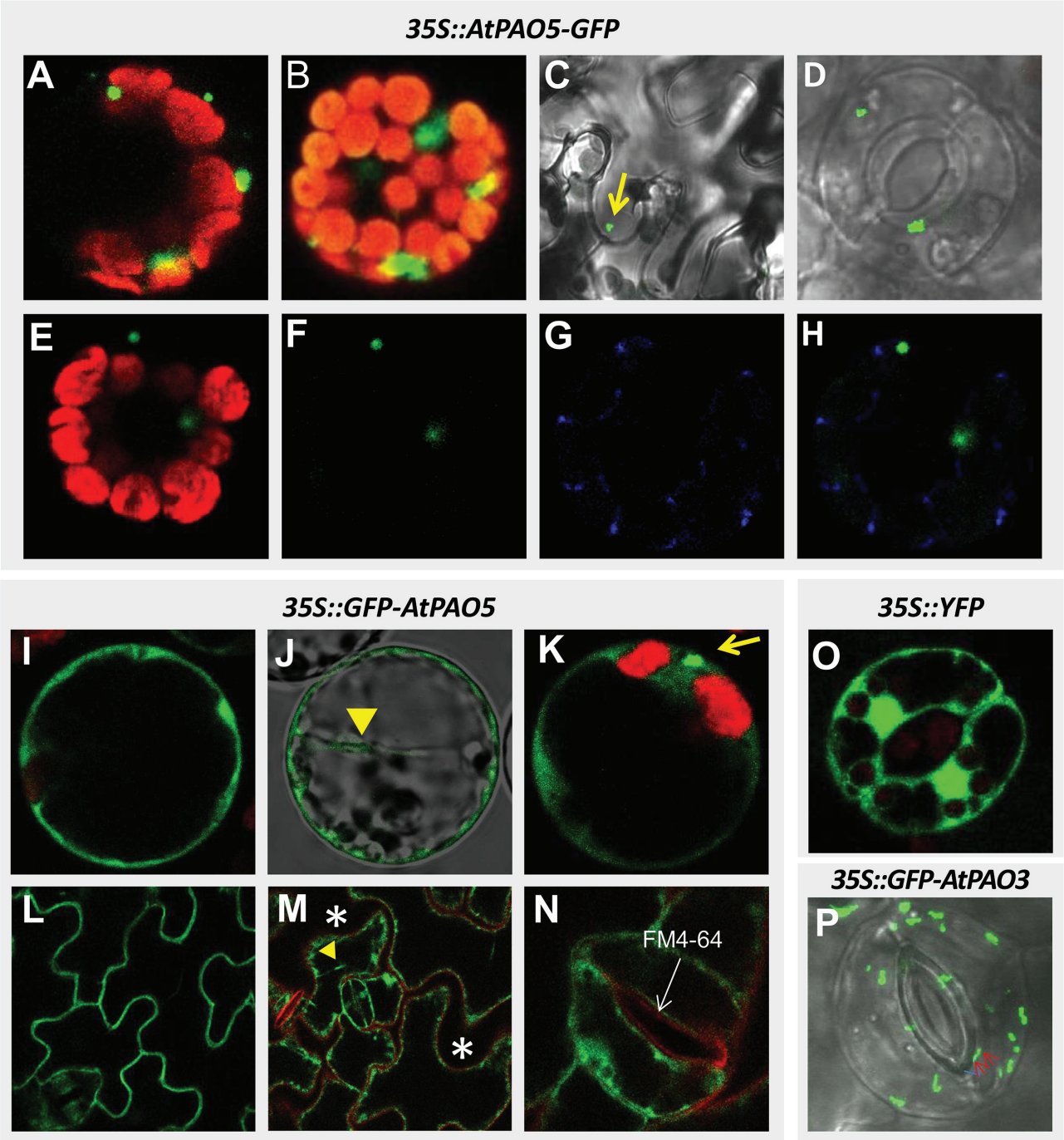

Fig. 5. Subcellular distribution of GFP-related fluorescence in the *35S::AtPAO5-GFP* and *35S::GFP-AtPAO5 Arabidopsis* transgenic plants. Confocal microscopy images of protoplasts and leaves of transgenic *Arabidopsis* plants stably expressing the *35S::AtPAO5-GFP* (A–H) and *35S::GFP-AtPAO5* constructs (I–N). As a control, confocal microscopy images of transgenic *35S::YFP* (O) and *35S::GFP-AtPAO3* (P) *Arabidopsis* plants are also shown. The fluorescence of GFP is shown in green. In A, B, E, and K, the autofluorescence of the chlorophyll is shown in red. In G and H, mitochondria stained by mitoTracker are shown in blue. H is a merged image of F and G. In M and N, the fluorescence of the membrane-specific dye FM4-64 is shown in red. In M, plasmolysed cells are shown, and white asterisks indicate areas between plasmolysed cells. Yellow arrows in C and K indicate the GFP-related fluorescent bodies, whereas the two red arrows in P show two sequential positions of a peroxisome undergoing rapid movement. Yellow arrowheads indicate cytosolic strands (J, M).

92.5%, but failed to detect the presence of UBQ, thus suggesting that the bulk amount of the recombinant AtPAO5-6His with the expected molecular weight is not ubiquitinated. In parallel, to examine further whether AtPAO5 undergoes polyubiquitination, the purified AtPAO5-6His protein was analysed by western blot using an anti-UBQ antibody. This analysis revealed the presence of high molecular weight proteins (80–130 kDa) recognized by the anti-UBQ antibody in two recombinant protein preparations which are absent in control preparations from wild-type plants (Fig. 8; white arrowheads). Conversely, the SDS–PAGE analysis did not reveal differences in the electrophoretic pattern between the

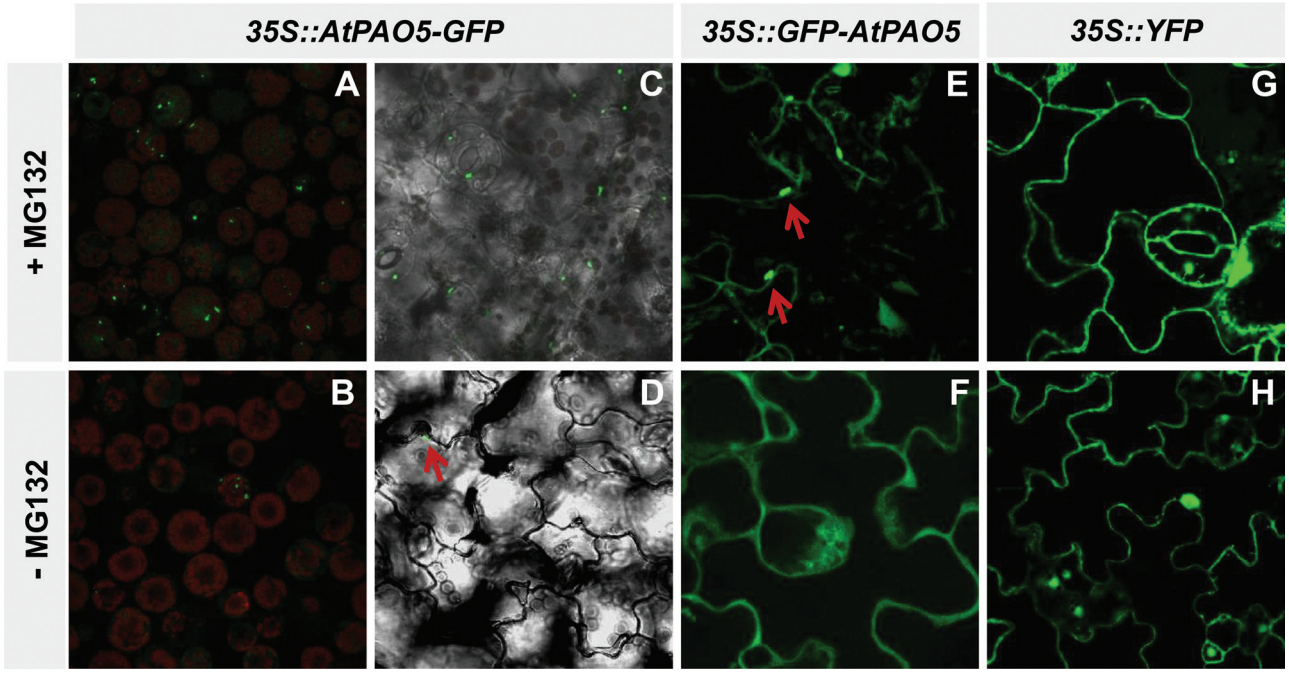

Fig. 6. Effect of the proteasome inhibitor MG132 on the distribution of GFP fluorescence in protoplasts and leaves from *35S::AtPAO5-GFP* and *35S::GFP-AtPAO5* transgenic *Arabidopsis* plants. Protoplasts (A, B) and leaves (C–H) from *35S::AtPAO5-GFP* (A–D), *35S::GFP-AtPAO5* (E, F), and *35S::YFP* transgenic (G, H) *Arabidopsis* plants were treated with 40 μM MG132 (+MG132; A, C, E, G) or 0.4% DMSO as a vehicle control (–MG132; B, D, F, H) for 16 h. Fluorescence of GFP is shown in green and autofluorescence of chlorophyll in red. Red arrows indicate some fluorescent bodies.

control and recombinant protein preparations in the high molecular weight region (Fig. 2). These data suggest that a small amount of the recombinant protein is ubiquitinated. The lack of high molecular weight signals in the western blot analysis using the anti-6His antibody (Fig. 7) may indicate that the 6His tag is hidden in the polyubiquitinated recombinant AtPAO5-6His protein or degraded. However, more data are still necessary to demonstrate unequivocally that the effect of proteasome on AtPAO5 protein stability is ubiquitin dependent.

AtPAO5 *expression levels are up-regulated by polyamines*

Spm treatment of *35S::GFP-AtPAO5* and *35S::AtPAO5-6His* transgenic *Arabidopsis* plants induced an increase in the levels of the recombinant proteins as compared with the untreated seedlings (Fig. 9), while no difference was observed at the corresponding mRNA levels as shown by qRT–PCR analysis (data not shown). In addition, no difference was observed in the accumulation levels of YFP in the *35S::YFP* transgenic plants following treatment with Spm (data not shown). These data indicate that Spm has an effect on recombinant AtPAO5 protein synthesis and/or stability. On the other hand, while analysis by qRT–PCR of the effect of Spm on the mRNA levels of the endogenous *AtPAO5* gene in wild-type plants showed no statistically significant difference between the Spm-treated and the untreated plants, analysis of *AtPAO5* promoter activity using *AtPAO5::GFP-GUS* *Arabidopsis* transgenic plants (Fincato *et al.*, 2012) showed that Spm brings about changes in *AtPAO5*-related GUS staining specifically in the root apex (Fig. 10). Conversely, no difference became evident in the above-ground part of the plant. In detail, while in the absence of any treatment, *AtPAO5*-related GUS staining was observed along the vascular system of the primary roots from the root–hypocotyl junction site up to the point in which the spiral/annular secondary cell wall thickenings of the protoxylem elements first become evident (Fig. 10A; Fincato *et al.*, 2012), Spm treatment increased the intensity of the GUS staining in the root apex, extending it up to the transition zone (TZ) between the meristematic and the elongation regions of the root (Fig. 10A). In agreement with these data, increased transcript levels of the *GUS* transgene were observed in the roots of the Spm-treated *AtPAO5::GFP-GUS* plants (Supplementary Fig. 4 at *JXB* online). A similar increase in GUS staining was also observed following treatment with Therm-Spm, which is in agreement with recent data from qRT–PCR showing that Therm-Spm increases *AtPAO5* expression levels (Marina *et al.*, 2013). In contrast to Spm and Therm-Spm, Spd and N^1-acetyl-Spm showed low efficiency to increase *AtPAO5* expression levels in the root apex (Fig. 10A). On the other hand, following treatment with Spm and Therm-Spm, but not with Spd and N^1-acetyl-Spm, GUS staining was absent in a short segment of the root differentiation zone proximal to the elongation region (Fig. 10B). These data altogether indicate that *AtPAO5* expression is regulated by polyamines at both the transcriptional and post-transcriptional level. At present, it is not known whether this regulatory effect is due to a direct effect of polyamines on the *AtPAO5* gene promoter and protein stability or to polyamine-mediated developmental changes. Indeed, Spm and Therm-Spm treatment shortened the distance between the first protoxylem elements with spiral cell wall thickenings and the apical meristematic

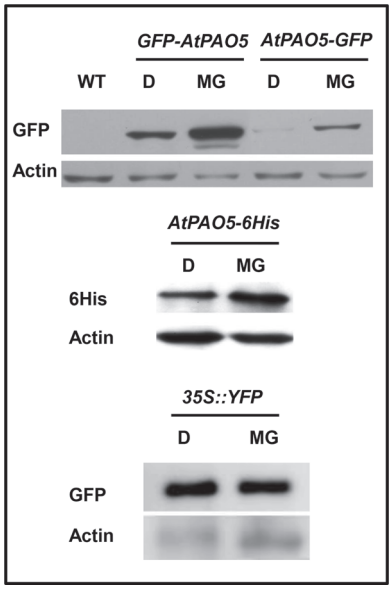

Fig. 7. Effect of the proteasome inhibitor MG132 on the accumulation levels of recombinant AtPAO5. Protein extracts from *35::GFP-AtPAO5*, *35S::AtPAO5-GFP*, *35S::AtPAO5-6His*, and *35S::YFP Arabidopsis* transgenic plants treated with 40 μM MG132 (MG) or 0.4% (v/v) DMSO (D) for 16 h were analysed by western blot using an anti-GFP or anti-6His antibody. Equal amounts of total proteins were subjected to SDS–PAGE, and actin was used as a loading control. WT, wild-type *Arabidopsis* plants. The experiment was repeated three times with similar results. A representative experiment is shown.

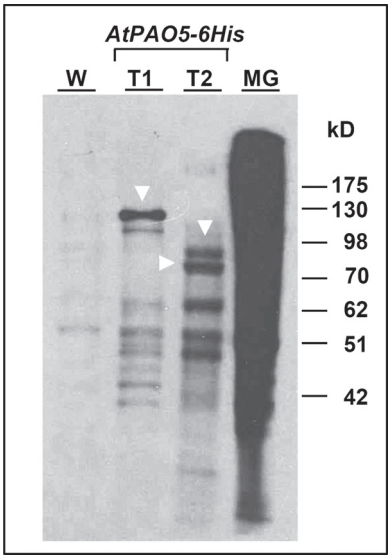

Fig. 8. Analysis of the ubiquitination state of recombinant AtPAO5-6His. Two independent preparations (T1, T2) of recombinant AtPAO5-6His from *35S::AtPAO5-6His Arabidopsis* plants obtained by affinity chromatography were analysed by western blot using an anti-UBQ antibody. A control preparation from wild-type plants (W) was also analysed. MG, total protein extract from wild-type plants treated with MG132. White arrowheads indicate putative polyubiquitinated forms of recombinant AtPAO5-6His. Numbers indicate the molecular weight of marker proteins (GeneDirex).

region, as determined by analysis of the *AtPAO5::GFP-GUS* transgenic plants using optical microscopy (Fig. 10C). Similar results were obtained for Spm by confocal analysis of wild-type plants (data not shown).

Discussion

The recent characterization of the catalytic properties of four out of five AtPAOs (AtPAO1, AtPAO2, AtPAO3, and AtPAO4) revealed important differences in substrate specificity among them, even among the three members of the AtPAO2–AtPAO4 subfamily (Tavladoraki *et al.*, 2006; Kamada-Nobusada *et al.*, 2008; Moschou *et al.*, 2008; Fincato *et al.*, 2011). It has also been demonstrated that these four AtPAOs are involved in polyamine back-conversion, in contrast to the extracellular PAOs of monocotyledonous plants which are involved in the terminal catabolism of polyamines, but similarly to the animal APAOs/SMOs. In the present study, it was shown that recombinant AtPAO5 bears a non-covalently bound molecule of FAD as a cofactor and that it oxidizes Spm and not Spd, consistent with its elevated sequence homology with MmSMO which specifically oxidizes Spm (Cervelli *et al.*, 2003). On the other hand, recombinant AtPAO5 is also active towards N^1-acetyl-Spm, the catalytic activity with this polyamine being 4-fold higher than that with Spm (Table 1) which is consistent with the high sequence similarity of AtPAO5 to MmAPAO. In this way, AtPAO5 represents the first plant enzyme characterized so far involved in polyamine catabolism with a good activity with this polyamine. Indeed, all other characterized plant PAOs have a much lower catalytic activity with the acetylated polyamines than with their free form. In particular, N^1-acetyl-Spm is a 5- to 300-fold poorer substrate than Spm for recombinant enzymes AtPAO1–AtPAO4 (Tavladoraki *et al.*, 2006; Fincato *et al.*, 2011) and is a non-competitive inhibitor of ZmPAO1 (Federico *et al.*, 1990).

Recombinant AtPAO5 is also active with Therm-Spm, and this is an important finding considering that Therm-Spm has an important role in plant defence responses (Sagor *et al.*, 2012; Marina *et al.*, 2013) and vascular system development (Clay and Nelson, 2005; Kakehi *et al.*, 2008, 2010; Rambla *et al.*, 2010; Vera-Sirera *et al.*, 2010; Milhinhos *et al.*, 2013) and that AtPAO5 is specifically expressed in the vascular system of the roots, the hypocotyls, and the stems (Fincato *et al.*, 2012). The catalytic activity of AtPAO5 towards Spm and Therm-Spm, but not at all towards Spd, makes it resemble AtPAO1 with which it also shares a similar subcellular localization (Tavladoraki *et al.*, 2006) and some common tissue-specific expression patterns, as, for example, in the anther tapetal cells and the anther–filament junction (Fincato *et al.*, 2012). These similarities between AtPAO1 and AtPAO5 permit the suggestion to be made that they have some common physiological roles, although the existing important differences between these two enzymes (i.e. regarding catalytic activity towards N^1-acetyl-Spm and expression in the vascular system) indicate some distinct physiological roles too.

Analysis of polyamine levels in the *35S::AtPAO5-6His* and *atpao5 Arabidopsis* plants showed that these plants have altered levels of Spm, Therm-Spm, and N^1-acetyl-Spm with respect to the wild-type plants, thus suggesting that

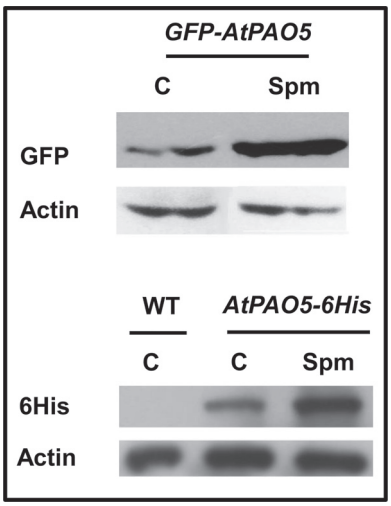

Fig. 9. Spm effect on the accumulation levels of GFP–AtPAO5 and AtPAO5–6His recombinant proteins in *Arabidopsis* transgenic plants. Protein extracts from *35::GFP-AtPAO5* and *35S::AtPAO5-6His Arabidopsis* plants treated with 0.5 mM Spm for 16 h were analysed by western blot using anti-GFP or anti-6His antibody. C, untreated control; WT, wild-type *Arabidopsis* plants. Equal amounts of total proteins were subjected to SDS–PAGE, and actin was used as a loading control. A representative experiment of three repetitions is shown.

these polyamines are also substrates of AtPAO5 *in vivo*. It should be noted, nevertheless, that the variations of Therm-Spm levels in the *35S::AtPAO5-6His* and *atpao5* plants are more relevant than those of Spm and N^1-acetyl-Spm, which may suggest that Therm-Spm is the best *in vivo* substrate of AtPAO5. However, more studies still have to be performed at different developmental stages, in various tissues/organs, and under different growth conditions for a better understanding of the substrate preference of this enzyme *in vivo*. These studies will also contribute to obtaining information about the physiological roles of the acetylated polyamines in plants, about which very little is known due to their presence at low levels (Tassoni *et al.*, 2000; Dufeu *et al.*, 2003; Hennion *et al.*, 2006) and to the fact that no information has been available so far about the enzymes involved in their metabolism in plants. Only recently has a role for plant acetylated polyamines in environmental stress responses been hypothesized (Hennion *et al.*, 2006). Acetylated polyamines are instead best known in animals and bacteria, where they constitute a significant part of the polyamine pool (Casero and Pegg, 1993). In animals, an important role for acetylated polyamines in homeostasis of intracellular polyamines has been proposed through their export and their degradation (Casero and Pegg, 2009). Acetylation is also used by *Escherichia coli* to reduce intracellular Spd levels in response to a variety of stress conditions (Tabor, 1968; Carper *et al.*, 1991). Furthermore, in addition to reducing the intracellular polyamine content, acetylation is considered to alter polyamine function also by preventing interaction with anionic sites in cellular macromolecules due to charge alteration (Casero and Pegg, 2009). The important role of acetylated polyamines in cellular metabolism is further evidenced by the fact that animal SSAT, the enzyme which catalyses the addition of acetyl groups to the aminopropyl end(s) of Spd and Spm, is highly regulated at multiple

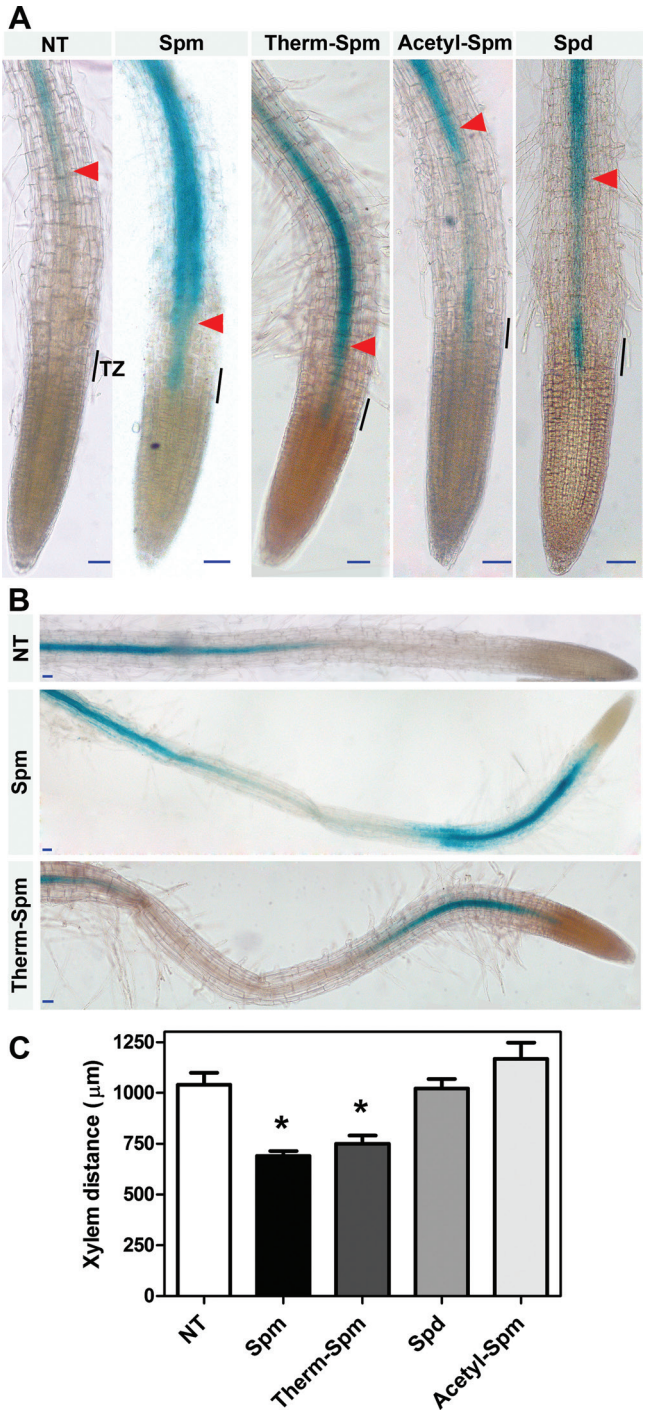

Fig. 10. Tissue-specific effect of exogenous polyamines on *AtPAO5* promoter activity and xylem differentiation. (A) Effect of Spm, Therm-Spm, N^1-acetyl-Spm, and Spd on *AtPAO5* promoter activity in root tips. Black lines indicate the transition zone (TZ) between the meristematic and the elongation regions of the root. (B) Effect of Spm and Therm-Spm on *AtPAO5* promoter activity in the root differentiation zone. GUS staining of *AtPAO5::GFP-GUS* transgenic seedlings treated or not with the various polyamines (0.5 mM) for 16 h. (C) Effect of polyamines on xylem differentiation. Five-day-old *AtPAO5::GFP-GUS Arabidopsis* seedlings were treated with 0.5 mM Spm, Therm-Spm, Spd, or N^1-acetyl-Spm for 16 h. Following tissue fixation and GUS staining, the distance between the first protoxylem elements with spiral cell wall thickenings (indicated by a red arrowhead) and the quiescent centre was measured using an optical microscope. Results are mean values ±SE. Asterisks indicate statistically significant differences as shown by one-way ANOVA test ($P<0.05$). The experiment was repeated twice with similar results. NT, not treated. Blue bars=50 µm.

levels by a variety of pathophysiological stimuli (Casero and Pegg, 2009).

The reactions catalysed by the flavin-dependent oxidoreductases use two half-reactions by which the flavin alternates between the oxidized and reduced states (Mattevi, 2006). In the reductive half-reaction, the substrate reduces the flavin, whereas in the oxidative half-reaction, the cofactor is re-oxidized by an electron acceptor. Flavin-dependent oxidases use molecular oxygen efficiently as electron acceptor to produce H_2O_2, whereas monooxygenases activate oxygen by forming a C4a-(hydro)peroxide of the flavin, which is then used to add an oxygen atom onto the substrate (Mattevi, 2006; Chaiyen *et al.*, 2012; Gadda *et al.*, 2012). Conversely, flavin-dependent dehydrogenases react slowly or not at all with O_2 and make use of other electron acceptors. The as yet characterized plant and animal PAOs have been shown to oxidize Spm and/or Spd efficiently using O_2 as an electron acceptor and producing H_2O_2 (Cervelli *et al.*, 2003; Polticelli *et al.*, 2006) and thus they are considered oxidases. An important finding of the present study is the observation that O_2 is a poor electron acceptor in the reaction catalysed by AtPAO5, the turnover rate being very low, as are the turnover rates of all PAOs so far characterized. Conversely, in the presence of artificial electron acceptors, such as ferricenium or ferricyanide, the k_{cat} values of AtPAO5 were similar to those of the other four AtPAOs and of the animal APAOs and SMOs characterized to date (Cervelli *et al.*, 2003; Wu *et al.*, 2003; Fincato *et al.*, 2011; Tavladoraki *et al.*, 2011). In this way, AtPAO5 can be classified as a spermine dehydrogenase and thus represents the first dehydrogenase to participate in polyamine catabolism in eukaryotes. Only in bacteria has the existence of spermidine dehydrogenases with an important role in the utilization of polyamines as carbon and nitrogen source been reported so far (Tabor and Kellog, 1970; Hisano *et al.*, 1990, 1992; Dasu *et al.*, 2006). Moreover, during preparation of the present manuscript, a study appeared online (Liu *et al.*, 2013) showing that OsPAO1, which is an AtPAO5 orthologue from *O. sativa* (Supplementary Table S1 at *JXB* online), has a very low k_{cat} value similar to that of AtPAO5 (present study) when calculated in the absence of any artificial electron acceptor (Table 1). These data suggest that all AtPAO5 orthologues have activity as spermine dehydrogenases. In the present study, it was also shown that ZmPAO1, in contrast to AtPAO5, has a 10-fold lower activity in the presence of ferricenium than only in the presence of O_2. These data confirm that ZmPAO1 has activity mainly as an oxidase and indeed its involvement in important physiological processes through production of H_2O_2 has been shown (Cona *et al.*, 2006; Angelini *et al.*, 2010; Tisi *et al.*, 2011). Instead, MmSMO was shown here to function both as an oxidase and as a dehydrogenase, the turnover rate in the presence of ferricenium being 54% that with only O_2. Although conditionally overexpression of MmSMO in the neocortex of transgenic mice resulted in increased production of H_2O_2 compared with the wild-type control mice (Cervelli *et al.*, 2013), the physiological relevance of its activity as a dehydrogenase has to be evaluated. Further studies have also to be performed to unravel the AtPAO5 native electron acceptor(s) which may allow the enzyme to achieve even higher turnover rates than those determined in the present study. Further studies have also to be undertaken to determine the physiological roles of AtPAO5. The function of AtPAO5 as a dehydrogenase and its involvement in polyamine back-conversion allows the suggestion of a role in polyamine homeostasis rather than in H_2O_2 production. This is further supported by the observation that AtPAO5 expression levels are regulated by polyamines.

The finding that AtPAO5 is involved in polyamine back-conversion, similarly to the other four AtPAOs, indicates that no PAO involved in the terminal catabolism of polyamines is present in *Arabidopsis*, in contrast to maize, barley, and rice plants in which both the polyamine back-conversion pathway and the terminal catabolic pathway are present (Fincato *et al.*, 2011; Ono *et al.*, 2012; Tavladoraki *et al.*, 2012). Considering the intracellular localization of all five AtPAOs, the conclusion can be drawn that the PAO-dependent polyamine back-conversion pathway is mostly intracellular, the terminal catabolic pathway being specifically active in the extracellular compartments (Fincato *et al.*, 2011). Thus, it is possible that in *Arabidopsis* only CuAOs contribute to polyamine terminal catabolism, which is consistent with the high number of *CuAO* genes in this plant, some of them with extracellular localization (Møller and McPherson, 1998; Wimalasekera *et al.*, 2011; Planas-Portell *et al.*, 2013).

Data from confocal microscopy and western blot analyses of the *35S::GFP-AtPAO5*, *35S::AtPAO5-GFP*, and *35S::AtPAO5-6His* transgenic plants suggest that AtPAO5 is a cytosolic protein regulated at the post-translational level by the proteasome, in agreement with the presence of putative PEST motifs for protein degradation in AtPAO5. They further show that the AtPAO5–GFP fusion protein is more susceptible to proteasome-dependent degradation than the recombinant GFP–AtPAO5 protein. Indeed, the AtPAO5-related fluorescent bodies were more frequently observed in the *35S::AtPAO5-GFP* plants than in *35S::GFP-AtPAO5* plants. Furthermore, the accumulation levels of the AtPAO5–GFP fusion protein in the plants with the highest expression levels were 10-fold lower than those of the AtPAO5–GFP fusion protein in the corresponding plants with a 1.5-fold difference at the corresponding mRNA levels (Supplementary Fig. S2 at *JXB* online). These data allow the exclusion of the possibility that the proteasome's effect on AtPAO5 protein accumulation is related to the high expression levels of the recombinant proteins and it can be hypothesized that the GFP at the N-terminus of AtPAO5 hides the putative PEST motif found proximally and protects the protein from degradation. This is the first time that such a regulatory mechanism has been proposed for a PAO. As regards polyamine metabolism in general, a similar regulatory mechanism has been shown only for animal ODC (Pegg, 2006) and SSAT (Coleman and Pegg, 2001). The physiological relevance of the proteasome-mediated regulation of *AtPAO5* expression has still to be determined. However, this finding suggests an important physiological role for AtPAO5 taking into consideration that the post-translational control is a characteristic of proteins that carry out critical cellular functions. It is likely that a cellular rapid response system is in place which limits either polyamine excess or insufficiency and controls changes in availability in response to demand.

Indeed, as shown in the present study, Spm treatment seems to increase recombinant AtPAO5 stability (Fig. 9).

This study showed that plant treatment with Spm and Therm-Spm increases *AtPAO5* promoter activity in the region between the TZ and the first protoxylem elements with spiral/annular cell wall thickenings (Fig. 10A). Furthermore, the same treatments bring about a decrease in *AtPAO5* promoter activity at a specific zone of the root differentiation/maturation region proximal to the root elongation region (Fig. 10B). In contrast to Spm and Therm-Spm, Spd and N^1-acetyl-Spm show low efficiency in affecting AtPAO5 expression levels in the same regions. Although the physiological significance of these observations is still unknown, they suggest a role for Spm and Therm-Spm and/or their catabolic products in *Arabidopsis* root development. Indeed, Spm and Therm-Spm, but not Spd and N^1-acetyl-Spm, were shown to reduce the distance of the first protoxylem elements with spiral/annular cell wall thickenings from the meristematic region (Fig. 10C). These data are in agreement with recent studies showing the role of polyamines in root development of different plant species, such as *P. antiscorbutica* (Hummel *et al.*, 2002) and *Z. mays* (Tisi *et al.*, 2011). However, these studies also highlight interspecies differences in the effect of the specific polyamines on plant development which merit further studies for a better comprehension of the underlying mechanisms.

In agreement with data presented here which indicate that Spm and Therm-Spm control AtPAO5 expression levels at both the transcriptional and post-transcriptional level, a root-specific effect of Spm and Therm-Spm on the expression levels of *OsPAO1*, the *AtPAO5* orthologue from *O. sativa* (Supplementary Table S1 at *JXB* online), has been reported very recently (Liu *et al.*, 2013). Although some differences apparently exist between *AtPAO5* and *OsPAO1*, such as for example regarding the specific expression pattern of *AtPAO5* in the root vascular tissue (Fincato *et al.*, 2012) whereas a more diffuse pattern was shown for *OsPAO1* (Liu *et al.*, 2013), the data from the two studies allow the suggestion that all *AtPAO5* orthologues are controlled by the same regulatory mechanisms in which polyamines and the proteasome-dependent degradation pathway are involved. Further studies are necessary to understand in detail the interplay between the polyamines and the proteasome complex, as well as the physiological importance of the above-mentioned regulatory mechanisms.

Supplementary data

Supplementary data are available at *JXB* online.

Figure S1. Analysis of AtPAO5 reaction products from Spm by TLC.

Figure S2. Analysis of *AtPAO5* expression levels in *35S::AtPAO5-GFP*, *35S::GFP-AtPAO5*, and *35S::AtPAO5-6His* transgenic plants.

Figure S3. Effect of the proteasomal inhibitor MG132 on protein ubiquitination in *Arabidopsis* plants.

Figure S4. Effect of Spm on *GUS* expression levels in roots of AtPAO5::GFP-GUS *Arabidopsis* plants.

Table S1. List of AtPAO5 orthologues

Acknowledgements

We are grateful to Plant Systems Biology (University of Gent) for the kind gift of the *pK2GW7*, *pK7FWG2*, and *pK7WGF2* binary vectors, and the Nottingham Arabidopsis Stock Centre for the SAIL_664_A11.v1 mutant. We also wish to thank Dr Alex Costa (University of Milan, Italy) for providing the *35S:: YFP Arabidopsis* plants, Professor Paolo Mariottini and Dr Manuela Cervelli (University 'Roma Tre', Rome, Italy) for providing recombinant MmPAO, as well as Professor Fabio Polticelli (University 'Roma Tre', Rome, Italy) and Dr Panagiotis N. Moschou (Swedish University of Agricultural Sciences and Linnean Center for Plant Biology, Uppsala, Sweden) for useful discussions. This work was implemented in the frame of COSTFA0605 action and was supported by the Italian Ministry of Education, University and Research (Project PRIN 2009WTCJL8_003), and University 'Roma Tre'.

References

Adachi MS, Taylor AB, Hart PJ, Fitzpatrick PF. 2012. Mechanistic and structural analyses of the role of His67 in the yeast polyamine oxidase Fms1. *Biochemistry* **51,** 4888–4897.

Alcázar R, Altabella T, Marco F, Bortolotti C, Reymond M, Koncz C, Carrasco P, Tiburcio AF. 2010. Polyamines: molecules with regulatory functions in plant abiotic stress tolerance. *Planta* **231,** 1237–1249.

Alet AI, Sánchez DH, Cuevas JC, Marina M, Carrasco P, Altabella T, Tiburcio AF, Ruiz OA. 2012. New insights into the role of spermine in *Arabidopsis thaliana* under long-term salt stress. *Plant Science* **182,** 94–100.

Aliverti A, Curti B, Vanoni MA. 1999. Identifying and quantitating FAD and FMN in simple and iron–sulfur-containing flavoproteins. *Methods in Molecular Biology* **131,** 9–23.

Angelini R, Cona A, Federico R, Fincato P, Tavladoraki P, Tisi A. 2010. Plant amine oxidases 'on the move': an update. *Plant Physiology and Biochemistry* **48,** 560–564.

Babbar N, Casero RA Jr. 2006.Tumor necrosis factor-alpha increases reactive oxygen species by inducing spermine oxidase in human lung epithelial cells: a potential mechanism for inflammation-induced carcinogenesis. *Cancer Research* **66,** 11125–11130.

Bianchi M, Amendola R, Federico R, Polticelli F, Mariottini P. 2005. Two short protein domains are responsible for the nuclear localization of the mouse spermine oxidase mu isoform. *FEBS Journal* **272,** 3052–3059.

Bloch D, Lavy M, Efrat Y, Efroni I, Bracha-Drori K, Abu-Abied M, Sadot E, Yalovsky S. 2005. Ectopic expression of an activated RAC in Arabidopsis disrupts membrane cycling. *Molecular Biology of the Cell* **16,** 1913–1927.

Burrell M, Hanfrey CC, Kinch LN, Elliott KA, Michael AJ. 2012. Evolution of a novel lysine decarboxylase in siderophore biosynthesis. *Molecular Microbiology* **86,** 485–499.

Carper SW, Willis DG, Manning KA, Gerner EW. 1991. Spermidine acetylation in response to a variety of stresses in *Escherichia coli*. *Journal of Biological Chemistry* **266,** 12439–12441.

Casero RA Jr, Pegg AE. 1993. Spermidine/spermine N^1-acetyltransferase—the turning point in polyamine metabolism. *FASEB Journal* **7,** 653–661.

Casero RA, Pegg AE. 2009. Polyamine catabolism and disease. *Biochemical Journal* **421,** 323–338.

Cervelli M, Bellavia G, D'Amelio M, *et al.* 2013. A new transgenic mouse model for studying the neurotoxicity of spermine oxidase dosage in the response to excitotoxic injury. *PLoS One* **8,** e64810.

Cervelli M, Bellini A, Bianchi M, Marcocci L, Nocera S, Polticelli F, Federico R, Amendola R, Mariottini P. 2004. Mouse spermine oxidase gene splice variants: nuclear sub-cellular localization of a novel active isoform. *European Journal of Biochemistry* **271,** 760–770.

Cervelli M, Polticelli F, Federico R, Mariottini P. 2003. Heterologous expression and characterization of mouse spermine oxidase. *Journal of Biological Chemistry* **278,** 5271–5276.

Chaiyen P, Fraaije MW, Mattevi A. 2012. The enigmatic reaction of flavins with oxygen. *Trends in Biochemical Sciences* **37,** 373–380.

Chattopadhyay MK, Hee PM, Tabor H. 2008. Hypusine modification for growth is the major function of spermidine in *Saccharomyces cerevisiae* polyamine auxotrophs grown in limiting spermidine. *Proceedings of the National Academy of Sciences, USA* **105,** 6554–6559.

Clay NK, Nelson T. 2005. Arabidopsis thickvein mutation affects vein thickness and organ vascularization, and resides in a provascular cell-specific spermine synthase involved in vein definition and in polar auxin transport. *Plant Physiology* **138,** 767–777.

Clough SJ, Bent AF. 1998. Floral dip: a simplified method for Agrobacterium-mediated transformation of *Arabidopsis thaliana*. *The Plant Journal* **16,** 735–743.

Coleman CS, Pegg AE. 2001. Polyamine analogues inhibit the ubiquitination of spermidine/spermine N^1-acetyltransferase and prevent its targeting to the proteasome for degradation. *Biochemical Journal* **358,** 137–145.

Cona A, Rea G, Angelini R, Federico R, Tavladoraki P. 2006. Functions of amine oxidases in plant development and defence. *Trends in Plant Science* **11,** 80–88.

Czechowski T, Stitt M, Altmann T, Udvardi MK, Scheible WR. 2005. Genome-wide identification and testing of superior reference genes for transcript normalization in Arabidopsis. *Plant Physiology* **139,** 5–17.

Dasu VV, Nakada Y, Ohnishi-Kameyama M, Kimura K, Itoh Y. 2006. Characterization and a role of *Pseudomonas aeruginosa* spermidine dehydrogenase in polyamine catabolism. *Microbiology* **152,** 2265–2272.

de Agazio M, Zacchini M, Federico R, Grego S. 1995. Putrescine accumulation in maize roots treated with spermidine: evidence for spermidine to putrescine conversion. *Plant Science* **111,** 181–185.

Dufeu M, Martin-Tanguy J, Hennion F. 2003. Temperature dependent changes of amine levels during early seedling development of the cold-adapted subantarctic crucifer *Pringlea antiscorbutica*. *Physiologia Plantarum* **118,** 164–172.

Federico R, Cona A, Angelini R, Schininà ME, Giartosio A. 1990. Characterization of maize polyamine oxidase. *Phytochemistry* **29,** 2411–2414.

Fellenberg C, van Ohlen M, Handrick V, Vogt T. 2012. The role of CCoAOMT1 and COMT1 in Arabidopsis anthers. *Planta* **236,** 51–61.

Fincato P, Moschou PN, Ahou A, Angelini R, Roubelakis-Angelakis KA, Federico R, Tavladoraki P. 2012. The members of *Arabidopsis thaliana PAO* gene family exhibit distinct tissue- and organ-specific expression pattern during seedling growth and flower development. *Amino Acids* **42,** 831–841.

Fincato P, Moschou PN, Spedaletti V, Tavazza R, Angelini R, Federico R, Roubelakis-Angelakis KA, Tavladoraki P. 2011. Functional diversity inside the Arabidopsis polyamine oxidase gene family. *Journal of Experimental Botany* **62,** 1155–1168.

Fuell C, Elliott KA, Hanfrey CC, Franceschetti M, Michael AJ. 2010. Polyamine biosynthetic diversity in plants and algae. *Plant Physiology and Biochemistry* **48,** 513–520.

Gadda G. 2012. Oxygen activation in flavoprotein oxidases: the importance of being positive. *Biochemistry* **51,** 2662–2669.

Gaquerel E, Kotkar H, Onkokesung N, Galis I, Baldwin IT. 2013. Silencing an *N*-acyltransferase-like involved in lignin biosynthesis in *Nicotiana attenuata* dramatically alters herbivory-induced phenolamide metabolism. *PLoS One* **8,** e62336.

Grienenberger E, Besseau S, Geoffroy P, Debayle D, Heintz D, Lapierre C, Pollet B, Heitz T, Legrand M. 2009. A BAHD acyltransferase is expressed in the tapetum of Arabidopsis anthers and is involved in the synthesis of hydroxycinnamoyl spermidines. *The Plant Journal* **58,** 246–259.

Groppa MD, Benavides MP. 2008. Polyamines and abiotic stress: recent advances. *Amino Acids* **34,** 35–45.

Hanfrey C, Elliott KA, Franceschetti M, Mayer MJ, Illingworth C, Michael AJ. 2005. A dual upstream open reading frame-based autoregulatory circuit controlling polyamine-responsive translation. *Journal of Biological Chemistry* **280,** 39229–39237.

Hanfrey C, Franceschetti M, Mayer MJ, Illingworth C, Michael AJ. 2002. Abrogation of upstream open reading frame-mediated translational control of a plant S-adenosylmethionine decarboxylase results in polyamine disruption and growth perturbations. *Journal of Biological Chemistry* **277,** 44131–44139.

Hennion F, Frenot Y, Martin-Tanguy J. 2006. High flexibility in growth and polyamine composition of the crucifer *Pringlea antiscorbutica* in relation to environmental conditions. *Physiologia Plantarum* **127,** 212–224.

Hisano T, Abe S, Wakashiro M, Kimura A, Murata K. 1990. Microbial spermidine dehydrogenase: purification and properties of the enzyme in *Pseudomonas aeruginosa* and *Citrobacter freundii*. *Journal of Fermentation and Bioengineering* **69,** 335–340.

Hisano T, Murata K, Kimura A, Matsushita, K, Adachi O. 1992. Further properties of spermidine dehydrogenase from *Citrobacter freundii* IFO 12681. *Bioscience, Biotechnology, and Biochemistry* **56,** 311–314.

Hummel I, Couée I, El Amrani A, Martin-Tanguy J, Hennion F. 2002. Involvement of polyamines in root development at low temperature in the subantarctic cruciferous species *Pringlea antiscorbutica*. *Journal of Experimental Botany* **53,** 1463–1473.

Ivanov IP, Atkins JF, Michael AJ. 2010. A profusion of upstream open reading frame mechanisms in polyamine-responsive translational regulation. *Nucleic Acids Research* **38,** 353–359.

Kakehi J-I, Kuwashiro Y, Motose H, Igarashi K, Takahashi T. 2010. Norspermine substitutes for thermospermine in the control of stem elongation in Arabidopsis thaliana. *FEBS Letters* **584,** 3042–3046.

Kakehi J, Kuwashiro Y, Niitsu M, Takahashi T. 2008. Thermospermine is required for stem elongation in *Arabidopsis thaliana*. *Plant and Cell Physiology* **49,** 1342–1349.

Kamada-Nobusada T, Hayashi M, Fukazawa M, Sakakibara H, Nishimura M. 2008. A putative peroxisomal polyamine oxidase, AtPAO4, is involved in polyamine catabolism in *Arabidopsis thaliana*. *Plant and Cell Physiology* **49,** 1272–1282.

Karimi M, Inzé D, Depicker A. 2002. GATEWAY vectors for Agrobacterium-mediated plant transformation. *Trends in Plant Science* **7,** 193–195.

Kim NH, Kim BS, Hwang BK. 2013. Pepper arginine decarboxylase is required for polyamine and γ-aminobutyric acid signaling in cell death and defense response. *Plant Physiology* **162,** 2067–2083.

Landry J, Sternglanz R. 2003. Yeast Fms1 is a FAD-utilizing polyamine oxidase. *Biochemical and Biophysical Research Communications* **303,** 771–776.

Law GL, Raney A, Heusner C, Morris DR. 2001. Polyamine regulation of ribosome pausing at the upstream open reading frame of S-adenosylmethionine decarboxylase. *Journal of Biological Chemistry* **276,** 38036–38043.

Lee DH, Goldberg AL. 1998. Proteasome inhibitors: valuable new tools for cell biologists. *Trends in Cell Biology* **8,** 397–403.

Lee J, Sperandio V, Frantz DE, Longgood J, Camilli A, Phillips MA, Michael AJ. 2009. An alternative polyamine biosynthetic pathway is widespread in bacteria and essential for biofilm formation in *Vibrio cholerae*. *Journal of Biological Chemistry* **284,** 9899–9907.

Lehman TC, Thorpe C. 1990. Alternate electron acceptors for medium chain acyl-CoA dehydrogenase: use of ferricenium salts. *Biochemistry* **29,** 10594–10602.

Liu T, Kim DW, Niitsu M, Berberich T, Kusano T. 2013. *Oryza sativa* polyamine oxidase 1 back-converts tetraamines, spermine and thermospermine, to spermidine. *Plant Cell Reports* (in press).

Mano S, Nakamori C, Hayashi M, Kato A, Kondo M, Nishimura M. 2002. Distribution and characterization of peroxisomes in Arabidopsis by visualization with GFP: dynamic morphology and actin-dependent movement. *Plant and Cell Physiology* **43,** 331–341.

Marina M, Sirera FV, Rambla JL, Gonzalez ME, Blázquez MA, Carbonell J, Pieckenstain FL, Ruiz OA. 2013. Thermospermine catabolism increases Arabidopsis thaliana resistance to *Pseudomonas viridiflava*. *Journal of Experimental Botany* **64,** 1393–1402.

Mattevi A. 2006. To be or not to be an oxidase: challenging the oxygen reactivity of flavoenzymes. *Trends in Biochemical Sciences* **31,** 276–283.

Mattoo AK, Minocha SC, Minocha R, Handa AK. 2010. Polyamines and cellular metabolism in plants: transgenic approaches reveal different responses to diamine putrescine versus higher polyamines spermidine and spermine. *Amino Acids* **38,** 405–413.

Michael AJ. 2011. Molecular machines encoded by bacterially-derived multi-domain gene fusions that potentially synthesize, N-methylate and transfer long chain polyamines in diatoms. *FEBS Letters* **585,** 2627–2634.

Milhinhos A, Prestele J, Bollhöner B, *et al.* 2013. Thermospermine levels are controlled by an auxin-dependent feedback loop mechanism in Populus xylem. *The Plant Journal* **75,** 685–698.

Møller SG, McPherson MJ. 1998. Developmental expression and biochemical analysis of the Arabidopsis atao1 gene encoding an H_2O_2-generating diamine oxidase. *The Plant Journal* **13,** 781–791.

Morimoto N, Fukuda W, Nakajima N, Masuda T, Terui Y, Kanai T, Oshima T, Imanaka T, Fujiwara S. 2010. Dual biosynthesis pathway for longer-chain polyamines in the hyperthermophilic archaeon *Thermococcus kodakarensis*. *Journal of Bacteriology* **192,** 4991–5001.

Moschou PN, Sanmartin M, Andriopoulou AH, Rojo E, Sanchez-Serrano JJ, Roubelakis-Angelakis KA. 2008. Bridging the gap between plant and mammalian polyamine catabolism: a novel peroxisomal polyamine oxidase responsible for a full back-conversion pathway in Arabidopsis. *Plant Physiology* **47,** 1845–1857.

Myung J, Kim KB, Crews CM. 2001. The ubiquitin–proteasome pathway and proteasome inhibitors. *Medicinal Research Reviews* **21,** 245–273.

Ober D, Gibas L, Witte L, Hartmann T. 2003. Evidence for general occurrence of homospermidine in plants and its supposed origin as by-product of deoxyhypusine synthase. *Phytochemistry* **62,** 339–334.

Okada M, Kawashima S, Imahori K. 1979. Substrate binding characteristics of the active site of spermidine dehydrogenase from *Serratia marcescens*. *Journal of Biochemistry* **85,** 1235–1243.

Ono Y, Kim DW, Watanabe K, Sasaki A, Niitsu M, Berberich T, Kusano T, Takahashi Y. 2012. Constitutively and highly expressed *Oryza sativa* polyamine oxidases localize in peroxisomes and catalyze polyamine back conversion. *Amino Acids* **42,** 867–876.

Oshima T. 2007. Unique polyamines produced by an extreme thermophile, *Thermus thermophilus*. *Amino Acids* **33,** 367–372.

Paik MJ, Lee S, Cho KH, Kim KR. 2006. Urinary polyamines and N-acetylated polyamines in four patients with Alzheimer's disease as their N-ethoxycarbonyl-N-pentafluoropropionyl derivatives by gas chromatography-mass spectrometry in selected ion monitoring mode. *Analytica Chimica Acta* **576,** 55–60.

Pegg AE. 2006. Regulation of ornithine decarboxylase. *Journal of Biological Chemistry* **281,** 14529–14532.

Pegg AE. 2008. Spermidine/spermine-N^1-acetyltransferase: a key metabolic regulator. *American Journal of Physiology – Endocrinology and Metabolism* **294,** E995–E1010.

Pegg AE. 2009. Mammalian polyamine metabolism and function. *IUBMB Life* **61,** 880–894.

Pegg AE, Michael AJ. 2010. Spermine synthase. *Cellular and Molecular Life Sciences* **67,** 113–121.

Penengo L, Mapelli M, Murachelli AG, Confalonieri S, Magri L, Musacchio A, Di Fiore PP, Polo S, Schneider TR. 2006. Crystal structure of the ubiquitin binding domains of rabex-5 reveals two modes of interaction with ubiquitin. *Cell* **124,** 1183–1195.

Planas-Portell J, Gallart M, Tiburcio AF, Altabella T. 2013. Copper-containing amine oxidases contribute to terminal polyamine oxidation in peroxisomes and apoplast of *Arabidopsis thaliana*. *BMC Plant Biology* **13,** 109.

Polticelli F, Basran J, Faso C, Cona A, Minervini G, Angelini R, Federico R, Scrutton NS, Tavladoraki P. 2005. Lys300 plays a major role in the catalytic mechanism of maize polyamine oxidase. *Biochemistry* **44,** 16108–16120.

Rambla JL, Vera-Sirera F, Blázquez MA, Carbonell J, Granell A. 2010. Quantitation of biogenic tetraamines in *Arabidopsis thaliana*. *Analytical Biochemistry* **397,** 208–211.

Raney A, Law GL, Mize GJ, Morris DR. 2002. Regulated translation termination at the upstream open reading frame in S-adenosylmethionine decarboxylase mRNA. *Journal of Biological Chemistry* **277,** 5988–5994.

Rea G, de Pinto MC, Tavazza R, Biondi S, Gobbi V, Ferrante P, De Gara L, Federico R, Angelini R, Tavladoraki P. 2004. Ectopic expression of maize polyamine oxidase and pea copper amine oxidase in the cell wall of tobacco plants. *Plant Physiology* **134,** 1414–1426.

Sagor GH, Takahashi H, Niitsu M, Takahashi Y, Berberich T, Kusano T. 2012. Exogenous thermospermine has an activity to induce a subset of the defense genes and restrict cucumber mosaic virus multiplication in *Arabidopsis thaliana*. *Plant Cell Reports* **31,** 1227–1232.

Seiler N. 2004. Catabolism of polyamines. *Amino Acids* **26,** 217–233.

Sessions A, Burke E, Presting G, *et al.* 2002. A high-throughput Arabidopsis reverse genetics system. *The Plant Cell* **14,** 2985–2994.

Tabor CW. 1968. The effect of temperature on the acetylation of spermidine. *Biochemical and Biophysical Research Communications* **30,** 339–342.

Tabor CW, Kellogg PD. 1970. Identification of flavin dinucleotide and heme in a homogeneous spermidine dehydrogenase from *Serratia marcescens*. *Journal of Biological Chemistry* **245,** 5424–5433.

Takahashi T, Kakehi J. 2010. Polyamines: ubiquitous polycations with unique roles in growth and stress responses. *Annals of Botany* **105,** 1–6.

Tassoni A, van Buuren M, Franceschetti M, Fornalè S, Bagni N. 2000. Polyamine content and metabolism in Arabidopsis thaliana and effect of spermidine on plant development. *Plant Physiology and Biochemistry* **38,** 383–393.

Tavladoraki P, Cervelli M, Antonangeli F, Minervini G, Stano P, Federico R, Mariottini P, Polticelli F. 2011. Probing mammalian spermine oxidase enzyme–substrate complex through molecular modeling, site-directed mutagenesis and biochemical characterization. *Amino Acids* **40,** 1115–1126.

Tavladoraki P, Cona A, Federico R, Tempera G, Viceconte N, Saccoccio S, Battaglia V, Toninello A, Agostinelli E. 2012. Polyamine catabolism: target for antiproliferative therapies in animals and stress tolerance strategies in plants. *Amino Acids* **42,** 411–426.

Tavladoraki P, Rossi MN, Saccuti G, Perez-Amador MA, Polticelli F, Angelini R, Federico R. 2006. Heterologous expression and biochemical characterization of a polyamine oxidase from Arabidopsis involved in polyamine back-conversion. *Plant Physiology* **141,** 1519–1532.

Tavladoraki P, Schininà ME, Cecconi F, Di Agostino S, Manera F, Rea G, Mariottini P, Federico R, Angelini R. 1998. Maize polyamine oxidase: primary structure from protein and cDNA sequencing. *FEBS Letters* **426,** 62–66.

Tisi A, Federico R, Moreno S, Lucretti S, Moschou PN, Roubelakis-Angelakis KA, Angelini R, Cona A. 2011 Perturbation of polyamine catabolism can strongly affect root development and xylem differentiation. *Plant Physiology* **157,** 200–215.

Tormos JR, Pozzi MH, Fitzpatrick PF. 2012. Mechanistic studies of the role of a conserved histidine in a mammalian polyamine oxidase. *Archives of Biochemistry and Biophysics* **528,** 45–49.

Vera-Sirera F, Minguet EG, Kumar S, Ljung K, Tuominen H, Blázquez MA, Carbonell J. 2010. Role of polyamines in plant vascular development. *Plant Physiology and Biochemistry* **48,** 534–539.

Vujcic S, Diegelman P, Bacchi CJ, Kramer DL, Porter CW. 2002. Identification and characterization of a novel flavin-containing spermine oxidase of mammalian cell origin. *Biochemical Journal* **367,** 665–675.

Vujcic S, Liang P, Diegelman P, Kramer DL, Porter CW. 2003. Genomic identification and biochemical characterization of the mammalian polyamine oxidase involved in polyamine back-conversion. *Biochemical Journal* **370,** 19–28.

Wang Y, Devereux W, Woster PM, Stewart TM, Hacker A, Casero RA Jr. 2001. Cloning and characterization of a human polyamine oxidase that is inducible by polyamine analogue exposure. *Cancer Research* **61,** 5370–5373.

White WH, Gunyuzlu PL, Toyn JH. 2001. *Saccharomyces cerevisiae* is capable of de novo pantothenic acid biosynthesis involving a novel pathway of β-alanine production from spermine. *Journal of Biological Chemistry* **276,** 10794–10800.

Wimalasekera R, Villar C, Begum T, Scherer GF. 2011. COPPER AMINE OXIDASE1 (CuAO1) of *Arabidopsis thaliana* contributes to abscisic acid- and polyamine-induced nitric oxide biosynthesis and abscisic acid signal transduction. *Molecular Plant* **4,** 663–678.

Wu T, Yankovskaya V, McIntire WS. 2003. Cloning, sequencing, and heterologous expression of the murine peroxisomal flavoprotein, N^1-acetylated polyamine oxidase. *Journal of Biological Chemistry* **278,** 20514–20525.